

NASA TECHNICAL MEMORANDUM

1N-72
64983

NASA TM-88500

P-97

KINETIC MODEL FOR THE VIBRATIONAL ENERGY EXCHANGE
IN FLOWING MOLECULAR GAS MIXTURES

F. Offenhäuser

Translation of "Kinetisches Modell für den Schwingungsenergie-
austausch in strömenden Molekülgasgemischen, University of
Stuttgart, West Germany, Aeronautics and Astronautics
Department, Dr.-Ing. Thesis, February 13, 1985, pp. 1-101
(A86-27827).

NATIONAL AERONAUTICS AND SPACE ADMINISTRATION
WASHINGTON, DC 20546 MARCH 1987

(NASA-TM-88500) KINETIC MODEL FOR THE
VIBRATIONAL ENERGY EXCHANGE IN FLOWING
MOLECULAR GAS MIXTURES Ph.D. Thesis
(National Aeronautics and Space
Administration) 97 p

N87-20802

Unclas
CSCL 20H G3/72 45218

1. Report No. NASA TM-88500		2. Government Accession No.		3. Recipient's Catalog No.	
4. Title and Subtitle KINETIC MODEL FOR THE VIBRATIONAL ENERGY EXCHANGE IN FLOWING MOLECULAR GAS MIXTURES				5. Report Date March 1987	
				6. Performing Organization Code	
7. Author(s) F. Offenhaeuser				8. Performing Organization Report No.	
				10. Work Unit No.	
				11. Contract or Grant No. NASW-4006	
9. Performing Organization Name and Address The Corporate Word, inc. 3 Gateway Ctr., 18 South Pittsburgh, PA 15222				13. Type of Report and Period Covered Translation	
				14. Sponsoring Agency Code	
12. Sponsoring Agency Name and Address National Aeronautics and Space Administration Washington, DC 20546					
15. Supplementary Notes Translation of "Kinetisches Modell fuer den Schwingungsenergie- austausch in stroemenden Molekuelgasgemischen, University of Stuttgart, West Germany, Aeronautics and Astronautics Department, Dr.-Ing. Thesis, February 13, 1985, pp. 1-101 (A86-27827).					
16. Abstract This study is concerned with the development of a computational model for the description of the vibrational energy exchange in flowing gas mixtures, taking into account a given number of energy levels for each vibrational degree of freedom. It is possible to select an arbitrary number of energy levels. The presented model uses values in the range from 10 to approximately 40. The distribution of energy with respect to these levels can differ from the equilibrium distribution. The kinetic model developed can be employed for arbitrary gaseous mixtures with an arbitrary number of vibrational degrees of freedom for each type of gas. The application of the model to CO ₂ -H ₂ O-N ₂ -O ₂ -He mixtures is discussed. The obtained relations can be utilized in a study of the suitability of radiation-related transitional processes, involving the CO ₂ molecule, for laser applications. It is found that the computational results provided by the model agree very well with experimental data obtained for a CO ₂ laser. Possibilities for the activation of a 16-micron and 14-micron laser are considered.					
17. Key Words (Selected by Author(s))				18. Distribution Statement Unlimited	
19. Security Classif. (of this report) Unclassified		20. Security Classif. (of this page) Unclassified		21. No. of Pages 97	
22. Price					

This paper came into being during my activities as a scientific employee at the Institute for Thermodynamics of Air- and Space Travel at the University of Stuttgart.

I thank Prof. Dr. A. Frohn for the theme of this dissertation, for the many liberties I enjoyed during that time, and for all the constructive discussions during a time when he himself had to deal with a great many burdens.

I thank Prof. Dr. W. A. Kreiner for his great interest which he showed so spontaneously in my work, as well as for the many comments and support which, at least in part, went beyond his task as associate reviewer.

I thank Prof. Dr. Hügel of the DFVLR Stuttgart and his co-workers for all the discussions which preceded this dissertation.

My thanks to all who were in any way helpful to me as this dissertation developed.

<u>Contents:</u>	Page
1. Introduction	5
2. General formulation of the reaction model	7
2.1. Rate equations and density distribution changes	7
2.2. Motion equations	11
2.3. Reaction velocity constants	13
2.3.1. Application of experimental results	15
2.3.2. Theoretical determination of kinetic data	25
2.4. Interferences of the Boltzmann Distribution	38
3. Application of the model on CO ₂ -H ₂ O-N ₂ -O ₂ -He Mixtures	42
3.1. Reaction system and numerical treatment	47
3.2. Overview over the kinetic data	55
3.3. Small signal amplification	58
3.4. Effect of superimposed radiation fields	61
4. Applications	63
4.1. Calculation of a cross-current CO ₂ -laser with HF-impulse	63
4.2. Examination of additional CO ₂ -laser crossings	69
4.3. Inversions in compression flow	75
5. Summary	78
Appendix:	
A Reaction velocity constants	79
A-1 Experimentally determined constants	79
A-2 Application of the Millikan-White Systematics	81
A-3 Application of Widom's Theory	83
B Electrical impulse coefficients	87
C Term scheme for the CO ₂ -H ₂ O-N ₂ -O ₂ - System	91
Literature cited	92

1. Introduction

The energy exchange between the inner and the outer degrees of freedom takes place during state changes in gases and gas mixtures; and it happens so fast that the details of the time-dependent events don't matter for many technical processes. This does not, however, apply for state changes when the gases become rarefied. When the pressure is sufficiently lowered, one can observe how, at first, the translational degrees of freedom of the molecules adjust to the new state and then, almost at the same time, the rotational degrees of freedom follow. The adjustment of the new vibrational state comes later in a most pronounced way. If one ignores the effect of radiation fields which may be present, then the changes in state are caused by the collisions of the molecules with one another. Thus, there are three possibilities for the change in the vibrational state. VT-collisions cause translational energy to be converted into vibrational energy. In the same manner, VR-collisions can cause rotational energy to be translated into vibrational degrees of freedom. These energy transfer processes are seldom differentiated experimentally which is why they are most often described in terms of VT-collisions. The third possibility for the energy exchange is given in terms of VV-collisions where a molecule can donate vibrational energy to the vibrational degrees of freedom of another molecule. As of today, many of these processes are not precisely understood. The vibrational energy exchange between various degrees of freedom is of technical interest wherever rarefied gases are encountered. This is often the case in space travel, for example, also for currents in shock tubes and wind tunnels. It is also in measuring techniques that these processes play an important role. For example, the results of laser fluorescence measurements can be influenced by the collision de-excitation of molecule vibrations. Some gases, furthermore, possess catalytic characteristics in their excited vibrational states with respect to chemical reactions. One of the most important areas of application, however, should be the development of molecular lasers.

While it is often possible to start from a momentary or localized energy equilibrium distribution for the translational- and the rotational degrees of freedom, even at substantial deviations from the thermodynamic equilibrium, one can just as frequently not justify this prerequisite for the degrees of vibrational freedom. The validity of such assumption must at least be carefully checked where energy transfer rates from VV-collisions reach the same magnitude as the energy transfer rates from VT-collisions. It is certain that there will be disturbances in the

Boltzmann distribution of the vibrational energy wherever there are strong radiation fields, as is the case in molecular lasers. In Chapter 4.2., CO₂-laser crossings are examined which could be activated only under the prerequisite that there is a disturbance in the Boltzmann distribution of the degrees of freedom.

The objective of this dissertation is the development of a mathematical model which describes the vibrational energy exchange in flowing gas mixtures. This will take into account a given number of energy levels for each vibrational degree of freedom. The number of these energy levels can be arbitrarily chosen. In the model chosen here, the values from 10 to 40 were used. The energy distribution beyond these levels can deviate from the equilibrium distribution.

In Chapter 4.1., the validity of the model is proven through the example of a so-called cross-current CO₂-laser with high-frequency excitation, for which experimental results from literature are available.

2. General Formulation

In this chapter, a kinetic model is developed which is applicable to any arbitrary gas mixtures with an arbitrary number of vibrational degrees of freedom per kind of gas. For the purpose of a more simplified, systematic treatment, the energy exchange reactions are divided into three categories:

- VT-collisions which lead to the energy transfer within the particular vibrational degrees of freedom.
- VV-collisions between different kinds of molecules.
- VV-collisions which lead to an equilibrium between two different vibrational degrees of freedom of a molecule.

For the purpose of better differentiation, the last category is going to be designated as the V-reaction in this paper. The VR-collisions are going to be assigned to the VT-collisions, as mentioned in the introduction.

2.1. Rate Equations and Density Distribution Changes

A gas mixture is considered which consists of N different types of gas. Each type of gas n shows I_n non-degenerated vibrational degrees of freedom with M energy levels. Degenerated vibrational forms are treated like simple degrees of freedom, but with twice the vibrational energy at a constant rate of transfer. Thus the number of VT-reactions between the ground state and the first excited vibrational state is given by

$$J = \sum_{n=1}^N I_n$$

and the total number of all VT-reactions is given by the product

$$J \cdot (M - 1)$$

In general, the reaction velocity constants for all molecule combinations will be different, so that one requires $J \cdot N$ velocity constants for all of the VT-reactions. From this, one can determine, as will be shown in Chapter 2.3.2., the velocity constants for vibrational energy levels of higher excitation and for all reactions in the opposite direction. In accordance with the division into the three reaction categories, there is a need for K reaction velocity constants for the VV-reactions. V-reactions may proceed, just like the VT-reactions, with any arbitrary collision partners, so that now there is a need for $L \cdot N$ velocity constants for L different V-reactions.

If the matrix of the concentration is designated as C , having J columns - corresponding to the total number of all vibrational degrees of freedom - and M lines - corresponding to the number of energy levels taken into account - , then one obtains for the concentration with respect to change with time

$$\frac{dC}{dt} = C \cdot \frac{1}{p} \cdot \frac{dp}{dt} + D \quad (2.1.-1)$$

The term $C \cdot \dot{p}/p$ taking into account the change in concentration due to change in density, and the matrix D which, like C , shows J columns and M lines, describes the transfer of matter in the reactions. There should be no significant gradients of the magnitudes of state perpendicular to the direction of flow, so that one deals with a uni-dimensional flow pattern. Matrix D is composed in accordance with the classification of reaction categories as follows:

$$D = A_{VT} \cdot D_{VT} + A_{VV} \cdot \vec{D}_{VV} + A_V \cdot \vec{D}_V \quad (2.1.-2)$$

Thus, all A_i numbers represent matrices which describe the qualitative transfer of matter in the reactions. Matrix D_{VT} contains all transfer rates of the VT-reactions in J columns and in $M-1$ lines, and vectors \vec{D}_{VV} and \vec{D}_V contain the K and L transfer rates of the remaining reactions. Matrix A_{VT} is put together in accordance with

$$a_{ji} = \begin{cases} -1 & \text{für } j = i \\ 0 & \text{für } j = i, i+1 \\ +1 & \text{für } j = i+1 \end{cases} \quad \begin{matrix} i = 1, 2, \dots, (M-1) \\ j = 1, 2, \dots, M \end{matrix}$$

The matrices A_{VV} and A_V , on the other hand, have a three-dimensional

structure which is shown in Fig. 2.1.-1. These matrices contain for certain values k, l at the location j, m the number 1 in space; this number has in the concentration matrix C an element $C_{j,m}$ which is formed in the reaction k, l ; they attain the number -1 , wherever there is in C an element $C_{j,m}$ which shows an initial substance in the same reaction k, l . All other matrix elements disappear.

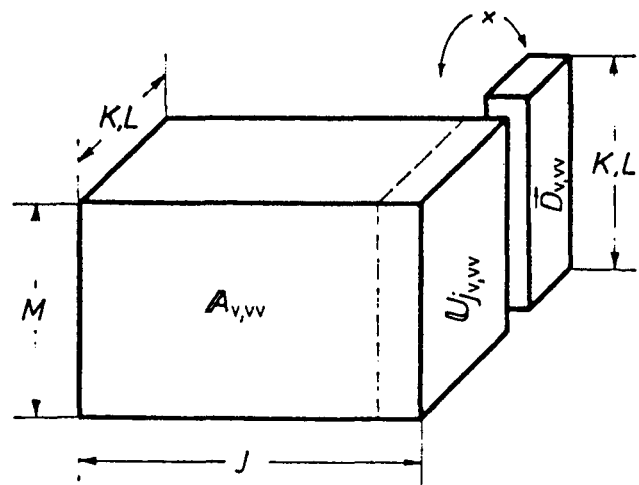


Fig. 2.1.-1

Structure of the reaction matrix A_v and A_{vv} .

Multiplying the transfer vector $\vec{D}_{v,vv}$ by sub-matrices $U_{jv,vv}$ leads to the plane transfer matrices $\vec{D}_{v,vv}$.

The multiplication with the transfer vectors $\vec{D}_{vv,v}$ has to be performed in such a way that each sub-matrix $U_{jvv,v}$ is multiplied by $\vec{D}_{vv,v}$. What results, is a matrix with J columns and M lines. The transfer rates of the VT-reactions which form the matrix D_{vT} are calculated according to

$$d_{vT}(j,m) = \sum_{n=1}^N \left\{ \bar{C}_n \cdot [H_{vT}(j,m,n) \cdot C_{j,m} - R_{vT}(j,m,n) \cdot C_{j,m+1}] \right\} \quad (2.1.-3)$$

where \bar{C}_n stands for the momentary total concentration of gas type n .

Since chemical reactions are not taken into account, \bar{C}_n changes only with

a change in density. The transfer rates of the remaining reactions which form the vector $\vec{D}_{VV,V}$, are calculated according to

$$d_{VV}(k) = H_{VV}(k) \cdot \prod_{a_{VV}(j,m,k)>0} C(j,m) - R_{VV}(k) \cdot \prod_{a_{VV}(j,m,k)<0} C(j,m) \quad (2.1.-4)$$

and

$$d_V(1) = \sum_{n=1}^N \left\{ C_n \cdot [H_V(1,n) \cdot C_A - R_V(1,n) \cdot C_B] \right\} \quad (2.1.-5)$$

The indices run from 1 to K,L. The designation C_A stands for those concentrations $C_{j,m}$ for which $a_V(j,m,1)>0$, and C_B stands for those concentrations for which $a_V(j,m,1)<0$. Generally, H stands for the reaction velocity constant of the endothermic reaction path and R stands for the constant of the opposite reaction. Quantum mechanics provides the connection between H and R as follows:

$$H = R \cdot \exp(-\Delta E/RT) \quad (2.1.-6)$$

Instead of concentrations, one frequently finds density distributions. The relationship between these two values is given by

$$n_m = C_m \cdot N_A$$

where n_m stands for the density distribution of a level m and N_A stands for Avogadro's constant. In cases of equilibria, the density distribution of levels of a vibrational degree of freedom are described by a Boltzmann distribution which is unequivocally determined by a given characteristic vibrational temperature Θ for the degree of freedom and by a momentary vibrational temperature T_{vib} . For the finite number M of energy levels, one obtains that portion of molecules situated in state m by the relationship

$$x_m = \frac{1 - \exp(-\Theta/T_{vib})}{1 - \exp[-(M+1) \cdot \Theta/T_{vib}]} \cdot \exp(-m \cdot \Theta/T_{vib}) \quad (2.1.-7)$$

where the index m can assume the values 0, 1, 2,, $M-1$.

For a Boltzmann distribution to exist, there is no need for thermodynamic equilibrium. With deviations from thermodynamic equilibrium, all degrees of freedom can qualify for a Boltzmann distribution where there is, in general, one particular local or momentary vibrational temperature T_{vib} for each vibrational degree of freedom. This is surely the case when the reaction velocity constants for the VV- and the V-reactions are substantially smaller than the velocity constants for the VT-reactions of the corresponding energy levels. One can, however, imagine cases where the Boltzmann distribution is disturbed by rapid VV- and V-reactions. This means that the complete coupled differential equation system must be solved, with the reaction-kinetic part given by equations (2.1.-1) through (2.1.-6).

2.2 Motion Equations

For cross-sectional changes, provided they don't occur too quickly, one can treat the flow of gas mixtures in a uni-dimensional form. Thus, the conservation equations for mass-, impulse-, and energy flow are

$$\rho \cdot u \cdot A = \rho_1 \cdot u_1 \cdot A_1 \quad , \quad (2.2.-1)$$

$$(\rho u^2 + p) \cdot A = (\rho_1 u_1^2 + p_1) \cdot A_1 \quad , \quad (2.2.-2)$$

$$\rho \cdot u \cdot A \left(h + \frac{1}{2} u^2 \right) = \rho_1 u_1 A_1 \left(h_1 + \frac{1}{2} u_1^2 \right) \quad . \quad (2.2.-3)$$

The designations p , u , and A stand for the momentary or local values of the gas density, for the flow velocity, and for the cross-sectional flow. The index 1 designates an initial state. In this paper, only flow in tubes with constant cross section is given consideration, so that

$$A = A_1$$

The density in the systems under consideration is so low that the thermal state equation for ideal gases

$$p = R \cdot \rho \cdot T$$

can be used. The change in enthalpy $\Delta h = h - h_1$ is developed in the form

$$\Delta h = \frac{7}{2} \alpha \cdot R \cdot (T - T_1) + \Delta e_{vib}$$

where Δe_{vib} is the change in the vibrational energy. The factor α takes care of the fact that eventually the admixed atomic gases will no longer possess any rotational degrees of freedom. If ψ_A is the mole fraction for molecular gases and ψ_B is the mole fraction for atomic gases in the mixture, then the relationship for the factor α is given by

$$\alpha = \psi_A + \psi_B \cdot 5/7$$

where $\psi_A + \psi_B = 1$ and $5/7 \leq \alpha \leq 1$. For time-related changes of the total density ρ , of the gas temperature T , and of the vibrational energy Δe_{vib} for the gas mixture, there are the following relationships with the help of the conservation equations:

$$\frac{d \Delta e_{vib}}{d t} = \frac{1}{\rho} \cdot \sum D_j \cdot E_j$$

$$\frac{d T}{d t} = \frac{d \Delta e_{vib}}{d t} / \left(\frac{R \cdot u^2}{u^2 - RT} - \frac{7}{2} \alpha R \right)$$

and

$$\frac{d \rho}{d t} = \frac{d T}{d t} \cdot R \cdot \rho / (u^2 - RT)$$

D_j stands for the transfer rate of reaction j , and E_j for its heat effect. For the flow velocity u , one immediately obtains $u = u_1 \cdot p_1 / p$ from the continuity equation.

2.3 Reaction Velocity Constants

One can, similar to chemical reactions, determine temperature-dependent velocity constants for the energy exchange between degrees of freedom in gases. Such quantities are measured. If this is not possible, then they have to be calculated theoretically. The application of reaction velocity constants for the energy exchange between the degrees of freedom in gases is not normally used. More often, one finds these processes characterized by relaxation times or transition probabilities. Transition probability $P_{n,m}$, obtained through a molecular velocity distribution, shows the probability at which a gas-kinetic collision of two particles evoke a change of the vibrational state from n to m of one of the two particles. With the help of quantum mechanics one can show that the exchange of more than one vibrational quantum per collision is relatively unlikely. In the same manner, one can show with the help of the kinetic gas theory that, at low densities and not excessively high temperatures, the collision of more than two particles is rare in comparison to the collision of two particles. This means that the distribution density change of any arbitrary energy level n of a degree of freedom can be described by the rate equation

$$\frac{dx_n}{dt} = Z \cdot (P_{n+1,n} \cdot x_{n+1} - P_{n,n+1} \cdot x_n + P_{n-1,n} \cdot x_{n-1} - P_{n,n-1} \cdot x_n) \quad (2.3.-1)$$

where Z stands for the frequency of collision of the given molecular velocity distribution. The following assumes that this is always a Maxwell velocity distribution. With the help of quantum mechanics, one obtains for the transition probabilities

$$P_{n+1,n} = (n+1) \cdot P_{1,0} \quad \text{and} \quad (2.3.-2)$$

$$P_{0,1} = P_{1,0} \cdot e^{-\Theta/T} \quad (2.3.-3)$$

where Θ stands for the characteristic vibrational temperature of the degree of freedom under consideration, and T stands for the gas temperature. By multiplying the distribution density change by the corresponding level energy

$\Delta e_n = R \cdot \Theta \cdot (n + 1/2)$, and by subsequent summation across all levels N , where N is finite, one obtains for the change in the total vibrational energy of the degree of freedom under consideration

$$\frac{d \Delta e_{vib}}{R \Theta \cdot d t} = Z \cdot P_{1,0} \cdot \left[(1 - \phi) \cdot \frac{\Delta \bar{e}_{vib} - \Delta e_{vib}}{R \Theta} + (N + 1) \cdot (N + \frac{3}{2}) \cdot \phi \cdot (\bar{x}_N - x_N) \right]$$

With the help of the statement

$$\frac{d \Delta e_{vib}}{d t} = \frac{\Delta \bar{e}_{vib} - \Delta e_{vib}}{\tau_{vib}}$$

one eventually obtains

$$\tau_{vib} = \frac{1}{Z \cdot P_{1,0} \cdot (1 - \phi) \cdot \psi} \quad (2.3.-4)$$

with

$$\psi = 1 + (N + 1) \cdot (N + \frac{3}{2}) \cdot \frac{\phi}{1 - \phi} \cdot (\bar{x}_N - x_N) \cdot R \Theta / (\Delta \bar{e}_{vib} - \Delta e_{vib})$$

N stands for the finite number of available energy levels, ϕ for the Boltzmann factor $\exp(-\Theta/T)$, and \bar{x}_N and $\Delta \bar{e}_{vib}$ stand for the uppermost energy level and for the oscillator energy in case of equilibrium. For the harmonic oscillator with $N \rightarrow \infty$, one obtains $\psi = 1$. For the harmonic oscillator with a finite number of levels N , one obtains, however, values of $\psi > 1$. For almost all gases, however, the approximation of $\psi = 1$ is valid for temperatures up to a few thousand degrees. Thus, the application of the pure exponential law within wide temperature limits appears justified, for the time being.

Since the kinetic data for the kinetic model of this paper are of great importance, a closer examination will now be conducted as to how these data can be determined.

2.3.1. Application of Experimental Results

If the results of the vibrational relaxation measurements are present in the form of relaxation times, they then can be used to calculate the corresponding reaction velocity constants. If the concentration of the collision partner is designated with $[M]$, then the effective velocity constant is obtained as

$$k = \frac{1}{\tau \cdot [M]} = \frac{Z}{[M]} \cdot (P_{1,0} - P_{0,1})$$

The velocity constant of the exothermic reaction results from it as

$$\frac{1}{k} = \frac{Z \cdot P_{1,0}}{[M]} \quad (2.3.1.-1)$$

From Equation (2.3.-4), one obtains for $P_{1,0}$ as the function of the relaxation time

$$Z \cdot P_{1,0} = \frac{1}{\tau \cdot (1 - \phi)}$$

with the Boltzmann factor $\phi = \exp(-\Theta/T)$, so that the velocity constant of the exothermic reaction assumes the term

$$\frac{1}{k} = \frac{R \cdot T}{\tau \cdot P_M \cdot (1 - \phi)} \quad (2.3.1.-2)$$

where P_M stands for the partial pressure of the collision partner.

Two methods for the measurement of VT-relaxation times have proven themselves as especially suitable:

- the measurement of the absorption of sound waves
- the measurement of the density structure in the relaxation zone behind gas-dynamic collisions.

Both methods are described in detail by *Cottrell* and *McCoubrey* [19]. Sound absorption measurements make a very accurate determination of the vibrational relaxation times possible at a relatively modest investment. For reasons related to application technology, this is, of course, possible only within a temperature region of 250 K and 1000 K. From the

sequence of sound absorption above the sound frequency, one can determine the vibrational relaxation time. The remarkable aspect of this method of measurement is that the deviations from thermodynamic equilibrium is always small. The measurements in the collision tube, on the other hand, make translational temperatures from 300 K to several 10000 K possible where substantial deviations from thermodynamic equilibrium can occur. From the density structure of the relaxation zone, one can determine the change of the inner energy of the gas. For most gases one can, without difficulty, calculate from this the share of vibrational energy, so that for each point of the relaxation zone one can determine a vibrational relaxation time. Measurements in CO_2 which were evaluated in this way, have shown that the distance from thermodynamic equilibrium exercises a significant influence upon the vibrational relaxation time [20]. This is also shown by the theoretical investigations in Chapter 2.3.2. of this paper. When VT-relaxation time measurements in molecular gases with several vibrational degrees of freedom are made, the problem arises that one either has to assign the gained relaxation times to a certain degree of freedom, or one has to split the results with the help of a model in order to obtain the relaxation times of all vibrational degrees of freedom. Next, simple models are used here to clarify the question, to what extent the particular VT-relaxation times of such molecules must differentiate themselves, so that they can be solved by sound absorption measurements or by density measurements in the collision tube. To this end it is assumed that within each vibrational degree of freedom there is a Boltzmann distribution, and that the vibrational degrees of freedom don't influence one another by couplings. Under those circumstances, one obtains the expression for the energy which is contained in the vibrational degrees of freedom, in terms of

$$e_{\text{vib}} = \sum_i e_{\text{vib}_i} = \sum_i R \theta_i \cdot \frac{\phi_i}{1 - \phi_i} \quad . \quad (2.3.1.-3)$$

Assuming that in the matter of sound waves in gases, one deals with adiabatic changes in state, one can describe the expansion of sound in accordance with *Cottrell, McCoubrey* [19] by

$$\frac{\partial \rho}{\partial t} + \rho \cdot \frac{\partial u}{\partial x} = 0 \quad ,$$

$$\frac{\partial u}{\partial t} + \frac{1}{\rho_0} \cdot \frac{\partial p}{\partial x} = 0 \quad ,$$

$$\frac{\partial e}{\partial t} - \frac{p}{\rho_0^2} \cdot \frac{\partial \rho}{\partial t} = 0 \quad ,$$

$$e = \frac{5}{2} RT + \sum_{i=1}^N e_{vib_i} \quad ,$$

$$\frac{\partial e_{vib_i}}{\partial t} = \frac{\bar{e}_{vib_i} - e_{vib_i}}{\tau_i} \quad .$$

An exponential expression of the type $f = f^* \cdot e^{-i(\omega t - kx)}$ for all variables results in a linear equation system whose solution leads to the complex velocity of sound

$$a = \left(\kappa \cdot \frac{p_0}{\rho_0} \right)^{1/2}$$

where κ is the complex adiabatic exponent which can be expressed by

$$\kappa = \frac{\frac{7}{2} + \sum_{j=1}^N \frac{c_{vib_j} / R}{1 - i \cdot \omega \cdot \tau_j}}{\frac{5}{2} + \sum_{j=1}^N \frac{c_{vib_j} / R}{1 - i \cdot \omega \cdot \tau_j}} \quad .$$

In this expression, $c_{vib_j} = \partial e_{vib_j} / \partial T$ is the heat capacity of the degree of freedom j at constant volume, $\omega = 2\pi\nu$ is the circular frequency of the sound wave, and τ_j is the VT-relaxation time of degree of freedom j . Thus, the following relationship is obtained for the velocity of sound as a function of frequency ν

$$c_s = \frac{1}{\operatorname{Re}(a^{-1})}$$

and for the absorption coefficient, one obtains

$$\alpha = 2\pi c_S \cdot \text{Im}(a^{-1}) \quad (2.3.1.-4)$$

The assumption is now made that the vibrational relaxation zone clearly contrasts from the pure gas-dynamic collision. Under this assumption, the vibrational relaxation zone can be described with the help of the conservation equations for mass-, impulse-, and energy flow at constant cross-sectional flow by

$$\begin{aligned} \rho \cdot w &= \rho_2 \cdot w_2 \quad , \\ \rho \cdot w^2 + p &= \rho_2 w_2^2 + p_2 \quad , \\ \rho \cdot w \left(\frac{1}{2} w^2 + \frac{7}{2} RT + e_{\text{vib}} \right) &= \rho_2 w_2 \left(\frac{1}{2} w_2^2 + \frac{7}{2} RT_2 + e_{\text{vib}_2} \right) \quad , \\ p &= \rho \cdot R \cdot T \quad , \\ e_{\text{vib}} - e_{\text{vib}_2} &= \sum_{i=1}^N \left[(e_{\text{vib}_3} - e_{\text{vib}_2}) \cdot (1 - e^{-t/\tau_i}) \right] \quad . \end{aligned}$$

The state immediately after the collision was characterized by the index "2", and the state of thermodynamic equilibrium was characterized by the index "3". If the equation system is solved for the dimensionless density $\gamma = p/p_2$, then one obtains

$$\gamma = \frac{1}{\frac{7}{12} \left(1 + \frac{1}{\kappa Ma_2^2} \right) + \left[\frac{1}{3 \kappa Ma_2^2} \cdot \sum_{i=1}^N \frac{e_{\text{vib}_3} - e_{\text{vib}_2}}{RT_2} \cdot (1 - e^{-t/\tau_i}) + \left(\frac{7}{12} \cdot \frac{1}{\kappa Ma_2^2} - \frac{5}{12} \right) \right]^{1/2}} \quad (2.3.1.-5)$$

The two equations (2.3.1.-4) and (2.3.1.-5) are now applied to carbon-dioxide and water vapor.

The CO₂-molecule exhibits the following vibrational forms:

- Symmetrical valence oscillation with $\theta_1 = 1920 \text{ K}$
- doubly decayed bending oscillation with $\theta_2 = 960 \text{ K}$
- asymmetrical valence oscillation with $\theta_3 = 3380 \text{ K}$

At a temperature of 288 K and a pressure of 1 bar, the vibrational relaxation time of CO₂ lasts about 6.13 μsec. It is now assumed that this

is the relaxation time of the bending oscillation, and then the question arises which common relaxation time the other two degrees of freedom have to show, so that one obtains a second relative maximum at the measurement of the sound absorption. Fig. 2.3.1.-1 shows that this is the case for the relaxation time relationships

$$\tau_{1,3} > 1000 \cdot \tau_2$$

Similar relationships result from weak collisions. At a temperature of 500 K immediately after the gas-dynamic collision and an initial pressure of 1 mbar, one should expect a vibrational relaxation time of 3.53 μ sec. One can see in Fig. 2.3.1.-3 that for the relaxation time relationships

$$\tau_{1,3} > 100 \cdot \tau_2$$

there is a step-wise density curve in the relaxation zone. If the temperature of 1000 K is chosen for both experiments, then the proof of varying relaxation times for

$$\tau_{1,3} > 100 \cdot \tau_2$$

is successfully made.

The H₂O-molecule exhibits the same vibrational forms as the CO₂-molecule:

- Symmetrical valence oscillation with $\theta_1 = 5257$ K
- simple bending oscillation with $\theta_2 = 2296$ K
- asymmetrical valence oscillation with $\theta_3 = 5406$ K

At a pressure of 1 mbar and a temperature of 288 K, the relaxation time is about 7.3 μ sec. It is assumed again, that this is the relaxation time for the bending oscillation, and then the question arises how large the common relaxation time of the other two oscillation forms have to be, so that two absorption maxima can be observed. This question is quickly answered by remembering that, according to equation (2.3.1.-3), the other two oscillation forms contain only 0.13% of the entire oscillation energy at a temperature of 288 K. This means that for the case at hand, one shouldn't expect a second absorption maximum, whatsoever. At the same temperature, the energy portion of the valence oscillations of the

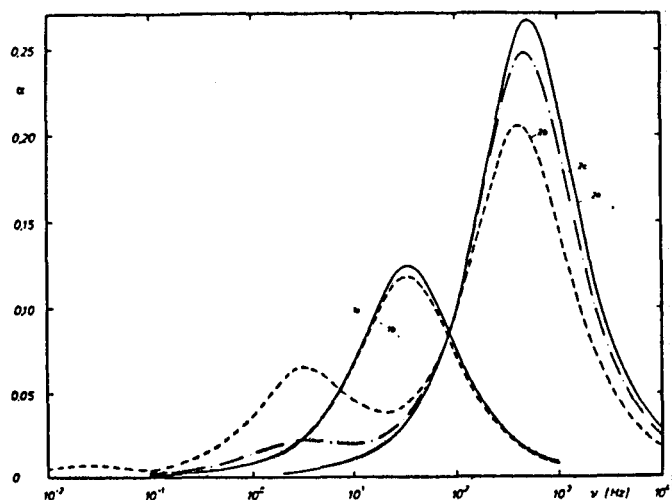


Fig. 2.3.1.-1

Sound absorption in CO_2 relative to $p = 1$ bar.

Curves designated with the numeral "1", refer to a temperature of 288 K.

1a: All degrees of freedom have the same relaxation time.

1b: Both valence oscillations have a relaxation time which is greater by a factor of 1000 than that of the deformation oscillation.

Curves designated with the numeral "2", refer to a temperature of 1000 K.

2a: All degrees of freedom have the same relaxation time.

2b: Both valence oscillations have a relaxation time which is greater by a factor of 100 than that of the deformation oscillation.

2c: The asymmetrical valence oscillation has a relaxation time which is greater by a factor of 100 than that of both other oscillation forms.

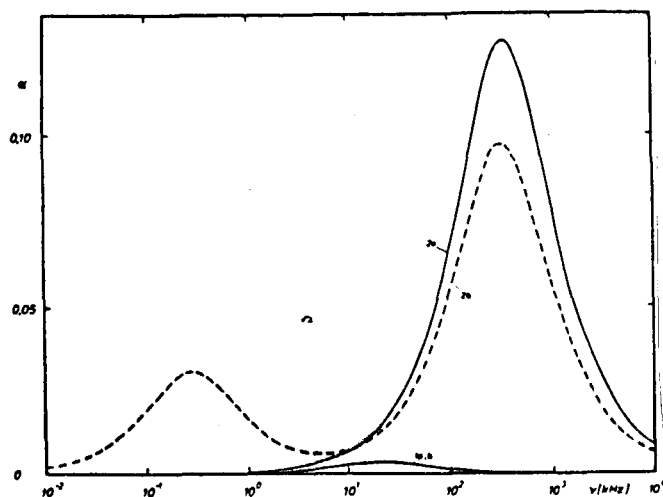


Fig. 2.3.1.-2

Sound absorption in H_2O relative to $p = 1$ bar.

Curves designated with the numeral "1", refer to a temperature of 288 K.

1a: All degrees of freedom have the same relaxation time.

1b: Both valence oscillations have a relaxation time which is greater by a factor of 1000 than that of the bending oscillation.

Curves designated with the numeral "2", refer to a temperature of 1000 K.

2a: All degrees of freedom have the same relaxation time.

2b: Both valence oscillations have a relaxation time which is greater by a factor of 1000 than that of the bending oscillation.

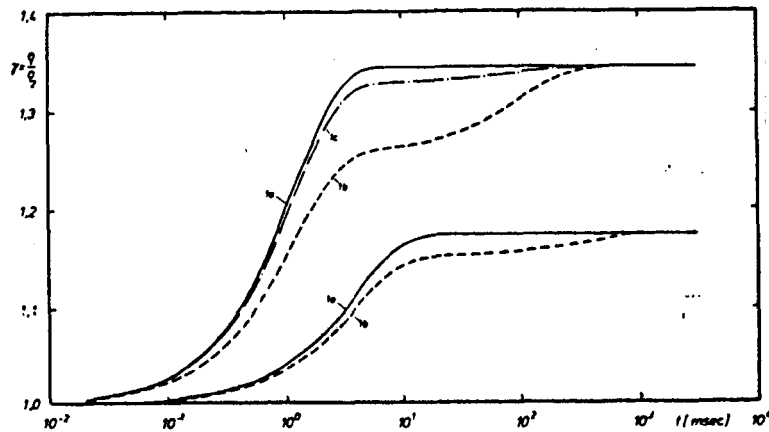


Fig. 2.3.1.-3

Density curves in the relaxation zone behind collisions in pure CO₂ at an initial pressure of 1 mbar.

The curves designated with the numeral "1" , refer to a collision Mach number of $Ma = 2.05$ and lead to a temperature of $T = 500$ K.

1a: All degrees of freedom have the same relaxation time.

1b: Both valence oscillations have a relaxation time which is greater by a factor of 100 than that of the deformation oscillation.

The curves designated with the numeral "2" , refer to a collision Mach number of $Ma = 3.6$ and lead to a temperature of $T = 1000$ K.

2a: All degrees of freedom have the same relaxation time.

2b: Both valence oscillations have a relaxation time which is greater by a factor of 100 than that of the deformation oscillation.

2c: The asymmetrical valence oscillation has a relaxation time which is greater by a factor of 100 than that of the deformation oscillation.

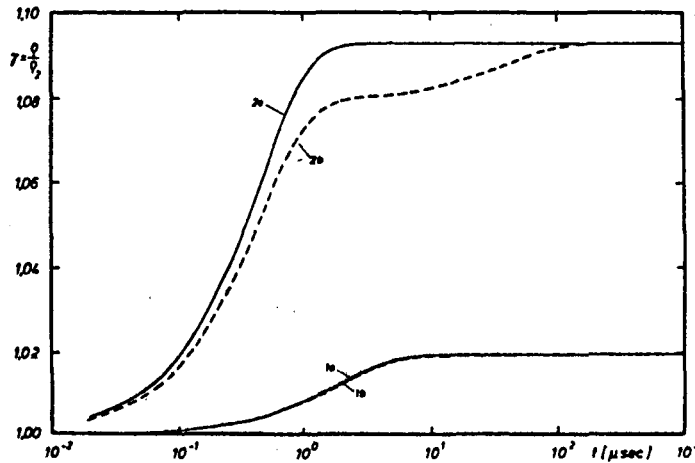


Fig. 2.3.1.-4

Density curves in the relaxation zone behind collisions in pure H_2O at an initial pressure of 1 mbar.

The curves designated with the numeral "1", refer to a collision Mach number of $\text{Ma} = 2.1$ and lead to a temperature of $T = 500 \text{ K}$.

1a: All degrees of freedom have the same relaxation time.

1b: Both valence oscillations have a relaxation time which is greater by a factor of 100 than that of the deformation oscillation.

The curves designated with the numeral "2", refer to a collision Mach number of $\text{Ma} = 3.5$ and lead to a temperature of $T = 1000 \text{ K}$.

2a: All degrees of freedom have the same relaxation time.

2b: Both valence oscillations have a relaxation time which is greater by a factor of 100 than that of the deformation oscillation.

CO₂-molecule was still 3.4%, in spite of the doubly decayed bending oscillation. The same thought can also find application for the relaxation zones after weak collisions; it also leads to the result that at low temperatures, a separate actuation of each particular degree of freedom can definitely not be observed with such experiments. Fig. 2.3.1.-2 and 2.3.1.-4 show that, at temperatures of about 1000 K, a solution for the degrees of freedom for both measuring methods becomes possible if

$$\tau_{1,3} > 100 \cdot \tau_2$$

From these investigations, one may conclude that the same relaxation time can not be assumed for all vibrational degrees of freedom of a molecule whenever the sound absorption measurements give only a relative maximum and whenever the collision tube experiments give no indication about a stepwise density curve in the relaxation zone. On the other hand, one can expect from spectroscopic measuring methods that a solution of the relaxation time for each particular vibrational degree of freedom is possible. Such investigations are difficult, however, because many of the necessary rotational oscillation transitions are of weak intensity, or they cannot be clearly identified due to overlaps. *Bethe* and *Teller* [1] do assume, however, that with molecules having several vibrational degrees of freedom, those vibrational forms are actuated fastest, which show the lowest characteristic vibrational temperatures. There also seem to be cases in which the vibrational forms with higher characteristic vibrational temperatures are preferably actuated. This was, for example, observed by *Ryali, et alii* [21] for the asymmetrical valence mode of CO₂ with N₂ as collision partner.

There are now numerous experimental results available for the relaxation time of the vibrational degrees of freedom of many gases. Often, error quotes are given for various experiments which lie far below the scatter of the experiments among one another. In the mean, the experiments scatter by a factor of two, where the deviations increase with an increase in the gas temperature. The details in Chapter 2.3. have shown that this cannot have anything to do with the actual limited number of energy levels for each vibrational degree of freedom. Based on this consideration, one can also exclude the influence of anharmonicities, because these begin to come into play only when very high energy levels are so tightly occupied

that they make a significant contribution to the vibrational energy of the respective degree of freedom. Consequently, it is easy to suspect that one deals with effects which can be traced to a dependence of the relaxation time upon the vibrational state or upon the deviation from the thermodynamic equilibrium. In the following chapter, it will be shown that both are valid.

2.3.2. Theoretical Calculation of the Kinetic Data.

For the theoretical calculation of kinetic data, it is necessary to determine the transition probability that corresponds to the vibrational excitation. If p is the transition probability for a single collision at a relative velocity g , then the median transition probability P is obtained by integration across the velocity distribution. When the transition probability P is multiplied by the number Z of the total gas-kinetic collisions, then the number of collisions is obtained that lead to a vibrational excitation in the medium. If P is known, then the corresponding relaxation times can be calculated according to Equation (2.3.1.-4), and the corresponding reaction velocity constants according to Equation (2.3.1.-1) or (2.3.1.-2).

Almost all theoretical calculations of the transition probability are based on quantum-mechanical expressions. With these methods of solution, the functions are substituted into the stationary or instationary Schrödinger equations, which are to describe the potential field in which the collision partners interact with one another. The transition probability p can be determined with the help of the exact or nearly-exact solutions for the Schrodinger equation. Closed solutions, however, exist only for certain, simple potential functions which often don't describe the real relationships very accurately. Obviously, the result of such calculations is, moreover, very dependent upon the form of the applied potential field. Nevertheless, it is possible to examine the solution circumstances in principle without committing to any particular potential field. The necessary quantum-mechanical calculations for this were carried out by *Döring* [2]. They are limited, however, to the harmonic oscillator with one degree of freedom. For the transition probability, one obtains on the basis of these calculations

$$p_{m \rightarrow n} = \frac{m!}{n!} \cdot e^{-|G|^2} \cdot \left| \sum_{j=0}^1 \left[\binom{n}{j} \cdot \frac{G^{n-j} \cdot (-G^*)^{m-j}}{(m-j)!} \right] \right|^2$$

The upper summation limit 1 is given by the smaller of the two values n and m which have the significance of vibrational quantum numbers. The quantity G will be designated as the interference function in the following description. It is obtained by a Fourier-transformation of force $F(t)$ which acts upon the oscillator whenever a collision occurs. In the following observations, the collisions are treated as nearly elastic. Consequently, the movement of particles during the collision becomes symmetrical with respect to the reversal point. Thus, the interference function now becomes

$$G = \frac{i}{\sqrt{2m\hbar\omega_0}} \cdot \int_{-\infty}^{+\infty} F(t) \cdot e^{i\omega_0 t} dt ,$$

which, by virtue of symmetry, is turned into a purely imaginary quantity. The conjugate-complex value G^* of the interference function is now equal to the negative value of the interference function itself. In this way, the transition probability is given by

$$p_{m \rightarrow n} = \frac{m!}{n!} \cdot e^{-|G|^2} \cdot \left| \sum_{j=0}^1 \left[\binom{n}{j} \cdot \frac{i^{n+m-2j} \cdot |G|^{n+m-2j}}{(m-j)!} \right] \right|^2 \quad (2.3.2.-1)$$

In most cases, the results in the region of the most frequent relative velocity of a Maxwell-velocity distribution are

$$|G| \ll 1 ,$$

and the relationship for the transition probability can be simplified, so that the result is

$$p_{m \rightarrow n} \approx \frac{m!}{n!} \cdot |G|^2 \quad (2.3.2.-2)$$

The collisions which occur at higher relative velocities, do not result in $|G| \ll 1$, but they are less frequent so that, in general, there is no large

error with respect to the median transition probability $P_{m \rightarrow n}$ at temperatures below about 1000 K. As can be seen from Equation (2.3.2.-2) the transition probability is largest for collisions, in which the vibrational quantum number changes by 1.

An estimate will now be made, how the median transition probability $P_{m \rightarrow n}$ depends upon the kinetic gas temperature. For this, the interference function G will first be determined.

As the potential field, a pure repulsive potential in the form of

$$v(r,y) = w_0 \cdot e^{-\alpha(r-\lambda y)}$$

is enlisted. In it, α stands for the stiffness of the potential and y stands for the vibration coordinate. The potential stiffness moves, for most gases, in a region of $2 \text{ \AA}^{-1} < \alpha < 5 \text{ \AA}^{-1}$. The vibration coordinate y can generally be neglected, compared to the action radius r , especially since $\lambda < 1$. Thus, the equation of motion of a central elastic collision

$$\mu \cdot \frac{d^2 r}{dt^2} = - \frac{dV(r)}{dr}$$

is obtained. μ stands for the reduced collision mass. With the limiting conditions $g(|t| \rightarrow \infty) = g_0$ and $r(|t| \rightarrow \infty) = \infty$, one obtains the solution

$$e^{-\alpha r} = \frac{\mu g_0^2}{2 w_0} \cdot \frac{1}{\cos h^2(\frac{\alpha}{2} g_0 t)}$$

With it, the relationship for the interference function is obtained as

$$|G| = \frac{2 \mu g_0 \lambda}{\sqrt{2 \pi \hbar \omega_0}} \cdot \frac{\frac{\pi \omega_0}{\alpha g_0}}{\sin h(\frac{\pi \omega_0}{\alpha g_0})}$$

The expression $\pi \omega_0 / \alpha g_0$ is, up to a numerical factor of the magnitude 1, equal to the quotient of the collision time and the duration of the oscillator's vibration. Therefore, the expression $\pi \omega_0 / \alpha g_0 \gg 1$ is valid for many applications, and by introducing of the approximation

$$\sin h(\frac{\pi \omega_0}{\alpha g_0}) \approx \frac{1}{2} e^{\frac{\pi \omega_0}{\alpha g_0}}$$

one can simplify the interference function, so that the relationship

$$|G| = \frac{4 \pi \mu \omega_0 \lambda}{\alpha \sqrt{2 \pi \hbar \omega_0}} \cdot e^{-\frac{\pi \omega_0}{\alpha g_0}}$$

is obtained. The portion of collisions which occurs at a relative velocity between g and $g + dg$, is

$$dZ = \left(\frac{\mu}{2KT}\right)^2 \cdot g_0^3 \cdot e^{-\frac{\mu}{2KT} g_0^2} dg_0$$

Thus, one obtains for the median transition probability

$$P = \int_0^{\infty} p(g_0) \cdot dZ(g_0)$$

and, along with Equation (2.3.2.-2), one finally winds up with

$$P = T^{-2} \cdot \int_0^{\infty} g_0^3 \cdot e^{-\frac{2\pi\omega_0}{\alpha g_0} - \frac{\mu}{2KT} g_0^2} dg_0$$

This integral cannot be solved in its closed form. The exponential function possesses, however, a sharp maximum at location

$$g^* = \left(\frac{2 \pi \omega_0 KT}{\alpha \mu}\right)^{1/3}$$

with the result for the temperature tendency being

$$P \sim T^{-1} \cdot e^{-\frac{3}{2} \left[\left(\frac{2\pi\omega_0}{\alpha}\right)^2 \cdot \frac{\mu}{KT} \right]^{-1/3}}$$

By neglecting a factor \sqrt{T} in relation to the factor of the temperature-dependent exponential function, one obtains for the temperature tendency

of the relaxation time

$$\ln \tau_{\text{vib}} \sim T^{-1/3}$$

This result was found using a different approach, back in 1936 by *Landau and Teller* [3], and was confirmed by numerous tests in a wide range of temperatures. The interference function could be simplified under the assumption that the vibration time of the oscillator is low compared to the collision time. The obtained temperature dependence of the relaxation time is also tied to this prerequisite. If the collision time is low compared to the vibration time, then the simplification

$$\sinh\left(\frac{\pi\omega_0}{\alpha g_0}\right) \approx \frac{\pi\omega_0}{\alpha g_0}$$

can be introduced which leads to the median transition probability

$$P = T^{-2} \cdot \int_0^{\infty} g_0^5 \cdot e^{-\frac{\mu}{2kT} g_0^2} dg_0 = \text{constant}$$

The temperature tendency for the relaxation time, in this case, then becomes

$$\tau_{\text{vib}} \sim T^{-1/2}$$

The stiffer the potential field and the smaller the oscillator frequency, the smaller the ratio between collision time and vibration time. The greatest effect, however, should be ascribed to the temperature. At an increasing temperature, the median relative velocity rises so that the collisions with $\tau_{\text{coll}}/\tau_{\omega_0} \ll 1$ gain in importance and that the temperature dependence of the relaxation time comes closer and closer to the pure root law. Under these circumstances, $|G| \ll 1$ is no longer valid. One must, therefore, examine what the effects are when consideration is given for the members of higher order in Equation (2.3.2.-1). The premise is kept that the collisions proceed in an almost elastic way. With these assumptions one obtains from Equation (2.3.2.-1) this relationship:

$$P_{n+1 \rightarrow n} = (n+1) \cdot e^{-|G|^2} \cdot \left\{ \sum_{j=0}^n \left[\binom{n+1}{j} \cdot \frac{(-1)^j \cdot |G|^{2j}}{(j+1)!} \right] \right\}^2 \cdot |G|^2$$

If the value of the interference function G does not grow beyond 0.4, then the number of the exponential function is always close to 1. Then one obtains as the approximation of the second order

$$p_{n+1 \rightarrow n} = (n+1) \cdot |G|^2 - n(n+1) \cdot |G|^4 + n^2(n+1) \cdot \frac{1}{4} |G|^6.$$

Averaged across the velocity distribution, one obtains

$$p_{n+1 \rightarrow n}^{(2)} = (n+1) \cdot p_{1 \rightarrow 0}^{(1)} - n(n+1) \cdot p_{1 \rightarrow 0}^{(1)} \cdot \varphi + n^2(n+1) \cdot p_{1 \rightarrow 0}^{(1)} \cdot \eta,$$

where the first order approximation is

$$p_{n+1 \rightarrow n}^{(1)} = (n+1) \cdot p_{1 \rightarrow 0}^{(1)}.$$

The defining equations for the factors φ and η are then

$$\varphi = \frac{\int_0^\infty f_{\text{Maxwell}}(g) \cdot |G|^4 dg}{\int_0^\infty f_{\text{Maxwell}}(g) \cdot |G|^2 dg}$$

$$\eta = \frac{1}{4} \cdot \frac{\int_0^\infty f_{\text{Maxwell}}(g) \cdot |G|^6 dg}{\int_0^\infty f_{\text{Maxwell}}(g) \cdot |G|^2 dg}.$$

For the chronological change of distribution densities, one thus obtains the relationship corresponding to Equation (2.3.-1)

$$\begin{aligned} \frac{dx_n}{dt} = Z \cdot P_{1,0}^{(1)} \cdot \left\{ \left[n \cdot \phi \cdot x_{n-1} - (n+(n+1) \cdot \phi) \cdot x_n + (n+1) \cdot x_{n+1} \right] \right. \\ \left. + \varphi \cdot \left[n(n-1) \cdot \phi \cdot x_{n-1} - (n(n-1) + n(n+1) \cdot \phi) \cdot x_n + n(n+1) \cdot x_{n+1} \right] \right. \\ \left. + \eta \cdot \left[n(n-1)^2 \cdot \phi \cdot x_{n-1} - (n(n-1)^2 + n^2(n+1) \cdot \phi) \cdot x_n + n^2(n+1) \cdot x_{n+1} \right] \right\} . \end{aligned}$$

For the chronological change of the vibrational energy, one obtains

$$\frac{de_{vib}}{dt} = R \cdot \theta \cdot \sum_{n=0}^{\infty} \left(n + \frac{1}{2} \right) \cdot \frac{dx_n}{dt}$$

after calculation of the sum and rearrangement of the members

$$\begin{aligned} \frac{de_{vib}}{dt} = Z \cdot P_{1,0}^{(1)} \cdot R \cdot \theta \cdot \sum_{n=0}^{\infty} \left\{ \left[(n+1) \cdot \phi - n \right] \right. \\ \left. - \varphi \cdot \left[n(n+1) \cdot \phi - n(n-1) \right] \right. \\ \left. + \eta \cdot \left[n^2(n+1) \cdot \phi - n(n-1)^2 \right] \right\} \cdot x_n . \end{aligned}$$

Here again, ϕ stands for the Boltzmann factor $\exp(-\theta/T)$. Under the assumption that there is always a Boltzmann distribution, the distribution densities are given by the relationship

$$x_n = (1 - \phi_v) \cdot \phi_v^n$$

In it, ϕ_v stands for the Boltzmann factor $\exp(-\theta/T_v)$, where T_v is the momentary vibration temperature. One thus obtains, after once more adding and rearranging the various members, the chronological change of the vibrational energy

$$\frac{de_{vib}}{dt} = Z \cdot P_{1,0}^{(1)} \cdot R \cdot \theta \cdot (1 - \phi) \cdot \left(\frac{\phi}{1 - \phi} - \frac{\phi_v}{1 - \phi_v} \right) \cdot \left[1 - \varphi \cdot \frac{2\phi_v}{1 - \phi_v} + \eta \cdot \frac{2(1 + 2\phi_v)}{1 - \phi_v} \right] .$$

Finally, if for $\phi/(1-\phi)$ the dimensionless equilibrium energy $e_{vib}/R\theta$ is substituted, and likewise the dimensionless momentary energy for $\phi_v/(1-\phi_v)$,

then one obtains

$$\frac{d e_{vib}}{dt} = Z \cdot p_{1,0}^{(1)} \cdot (1-\phi) \cdot (\bar{e}_{vib} - e_{vib}) \cdot \left[1 - \gamma \cdot 2 \frac{e_{vib}}{R\theta} + \eta \cdot 2(1+3 \frac{e_{vib}}{R\theta}) \right] .$$

Thus the precise result for the vibrational relaxation time in the approximation of the second order is the relationship

$$\tau_{vib}^{(2)} = \frac{1}{Z \cdot p_{1,0}^{(1)} \cdot (1-\phi) \cdot \left[1 - \gamma \cdot 2 \frac{e_{vib}}{R\theta} + \eta \cdot 2(1+3 \frac{e_{vib}}{R\theta}) \right]} ,$$

while the result of the first approximation is

$$\tau_{vib}^{(1)} = \frac{1}{Z \cdot p_{1,0}^{(1)} \cdot (1-\phi)}$$

According to Equation (2.3.2.-3), the vibrational relaxation time depends not only on the gas temperature, but also on the momentary state of oscillation. With this condition, one can explain the temperature-increase-related, rising width of scatter of the experimental results. An especially large deviation must, therefore, be suspected between experimental results which were obtained with the collision tube- and sound absorption methods, because with the sound absorption method, the deviations from the equilibrium are weak, but with the collision tube method, the deviations can be very large. This effect can be easily proven from literature. The available results of both measuring methods cross in a temperature region of about 500 K to 1000 K . With the aid of Equation (2.3.2.-3), one can now determine the quotient of the actual momentary relaxation time τ and the relaxation time $\bar{\tau}$ for minor deviations from equilibrium at equal gas temperature. One obtains

$$\frac{\tau}{\bar{\tau}} = \frac{1 - \gamma \cdot 2 \epsilon + \eta \cdot 2(1+3 \epsilon)}{1 - \gamma \cdot 2 \bar{\epsilon} + \eta \cdot 2(1+3 \bar{\epsilon})} .$$

Here, ϵ is the oscillation energy, standardized with $R\theta$. For most gases, one obtains $\gamma > 3\eta$ in the valid region of this approximation. In this case, $\tau/\bar{\tau} < 1$ is always valid, independent of ϵ and $\bar{\epsilon}$.

The exchange of energy between translational- and vibrational degrees of freedom takes place so much more rapidly, the farther the system is away from equilibrium. This was also observed by *Hurle* [4] in expansional flow of nitrogen, and by *Johannesen, et alii* [5] in the relaxation zone after gas-dynamic collisions in CO_2 -gas at collision Mach numbers between 1.4 and 4. For large values of the interference function G , the approximation of the second order also loses its validity. Equation (2.3.2.-3) can then no longer be applied, since the integration of the transition probability across the Maxwell distribution takes place, to a large extent, in velocity regions where the quantity of the interference function G exceeds the value of 0.4. This happens when the gas temperature exceeds a certain value which, for example, for the deformation oscillation of CO_2 comes to about 700 K. Beyond this limit, one would have to take terms of a higher order into account which would necessitate an effort that would no longer justify an analytical solution. For $|G| \gg 0.4$, the transition probability does not, however, climb monotonously, but it shows a resonance structure as presented in Fig. 2.3.2.-1 for the bending oscillation of the CO_2 -molecule.

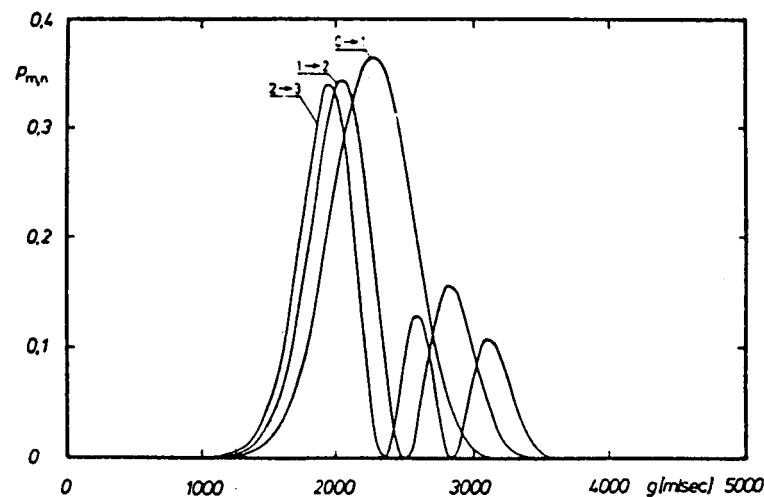


Fig. 2.3.2.-1

Graph of the transition probability for the deformation oscillation of CO_2 over the relative velocity.

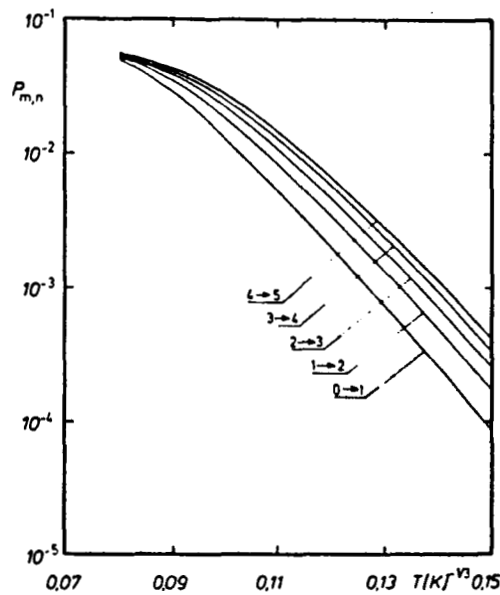


Fig. 2.3.2.-2

Graph of the median transition probability for the deformation oscillation of CO_2 over the gas temperature.

As can be seen from Fig. 2.3.2.-2, one does not obtain any more

$$P_{n+1,n} = (n+1) \cdot P_{1,0} ,$$

for the median transition probability at high temperatures but rather, in approximation

$$P_{n+1,n} = P_{1,0}$$

This opens the possibility for the examination of the dependence of the relaxation time on the gas temperature and on the oscillation state, even at higher temperatures. In order to remain general, the following will have to be understood in terms of temperatures which are several times the characteristic oscillating temperature. From Equation 2.3.-1, one obtains the relationship

$$\frac{dx_n}{dt} = Z \cdot P_{1,0} \cdot [x_{n+1} - (1+\phi) \cdot x_n + \phi \cdot x_{n-1}] \quad (2.3.2.-4)$$

After multiplication by level energy $e_{vib(n)} = R \cdot \theta \cdot (n + 1/2)$ and adding across n from 0 to ∞ , one obtains

$$\frac{de_{vib}}{dt} = Z \cdot P_{1,0} \cdot R \cdot \theta \cdot [x_0 - (1-\phi)]$$

The differential quotient disappears for $x_0 = 1 - \phi$, which is a sufficient enough condition for applying the Boltzmann distribution. By employing the Boltzmann distribution $x_n = (1 - y) \cdot y^n$ in Equation (2.3.2.-4), one obtains

$$[n(1-y) - y] \cdot \dot{y} = Z \cdot P_{1,0} \cdot (1-y) \cdot [y^2 - (1+\phi) \cdot y + \phi]$$

In the state of equilibrium, the left side of the equation disappears since $\dot{y} = 0$, and one obtains, with the aid of the right side of the equation, the only physically meaningful solution $y = \phi$. This means that at the beginning and toward the end of the change in state, there is a Boltzmann distribution. During the change in state, there can be no Boltzmann distribution, because the left side of the equation has the oscillation quantum number n , and the term in the large bracket does not disappear. From the foregoing considerations, the relaxation times can now be given at the beginning and at the end of the relaxation zone without the necessity for solving the differential equation for distribution density. For the beginning of the relaxation there is with

$$\tau_{vib(0)} = \frac{e_{vib} - e_{vib(0)}}{\left(\frac{de_{vib}}{dt}\right)_0}$$

the relationship

$$\tau_{vib(0)} = \frac{1}{Z \cdot P_{1,0} \cdot (1-\phi) \cdot (1-\phi_0)}$$

and toward the end of the relaxation with

$$\tau_{vib}(\infty) = \lim_{e_{vib} \rightarrow \bar{e}_{vib}} \frac{\bar{e}_{vib} - e_{vib}}{\frac{d e_{vib}}{d t}}$$

the relationship

$$\tau_{vib}(\infty) = \frac{1}{Z \cdot p_{1,0} \cdot (1 - \phi)^2} \cdot$$

ϕ_0 stands for the Boltzmann factor at the beginning of the relaxation and ϕ stands for the Boltzmann factor which is formed with the gas temperature. At an equal gas temperature, the following relationship results for the quotient of $\tau_{vib}(0)$ and $\tau_{vib}(\infty)$:

$$\frac{\tau_{vib}(0)}{\tau_{vib}(\infty)} = \frac{1 - \phi}{1 - \phi_0} \cdot$$

If one uses the corresponding vibrational energies in place of the Boltzmann factors, then the result for the relaxation time at the beginning of the process is

$$\tau_{vib}(0) = \frac{1}{Z \cdot p_{1,0} \cdot (1 - \phi)} \cdot \frac{\frac{e_{vib}(0)}{R\theta}}{1 + \frac{e_{vib}(0)}{R\theta}} \quad (2.3.2.-5)$$

and for the relaxation time quotient, it is

$$\frac{\tau_{vib}(0)}{\tau_{vib}(\infty)} = \frac{\epsilon(0)}{\epsilon(\infty)} \cdot \frac{1 + \epsilon(\infty)}{1 + \epsilon(0)} \cdot$$

where ϵ stands for the dimensionless oscillation energy $e_{vib}/R\theta$. In contrast to Equation (2.3.2.-3), there are always varying results for compressional and expansional flow with Equation (2.3.2.-5). According to Equation (2.3.2.-5) there is always, at high temperatures after compressional collisions, a relaxation time which is smaller than the relaxation time at a slight deviation from the equilibrium. For expansional flow there is, however, always an increase in the relaxation time. Experiments in the collision tube have confirmed this behavior [20].

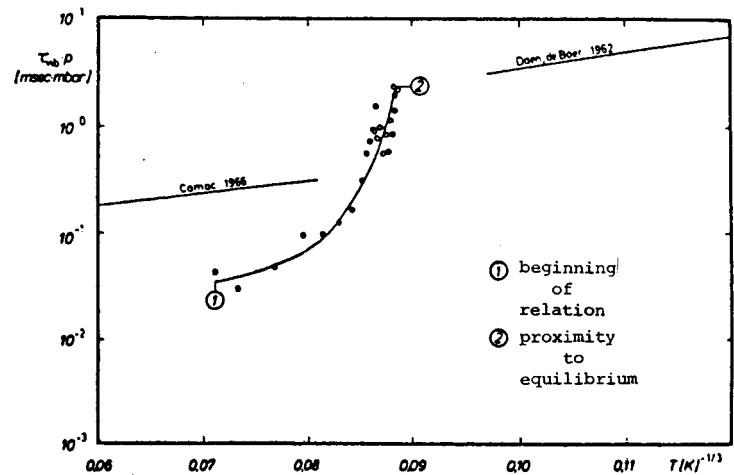


Fig. 2.3.2.-3

Graph of the relaxation time after a collision in pure CO_2 at a collision Mach number of $\text{Ma} = 5.01$, an initial pressure of 0.3 mbar, and an initial temperature of 293 K.

In Fig. 2.3.2.-3, one can see a typical graph of the relaxation time across the relaxation zone for the bending oscillation of the CO_2 -molecule. At the beginning of the relaxation, the relaxation time is still definitely smaller, as expected from earlier results. Toward the end of the relaxation, on the other hand, relaxation times are measured which show good agreement with earlier results. According to Equation (2.3.2.-3), the deviations of the relaxation time from the relaxation time at slight interferences are the larger, the smaller the characteristic oscillation temperature of the corresponding degree of freedom is. This appears to explain why the relaxation time measurements in CO_2 show an increasing scatter with an increase in the gas temperature. Because of the relatively low characteristic temperature of the bending oscillation of 960 K, one must expect deviations in the relaxation time at slight interferences which can reach one order of magnitude or more. There is only little known from published literature, where the changes in the relaxation time on account of the decrease in gas temperature in the relaxation zone are considered. Many measurements, therefore, deal with a median value for the entire relaxation zone.

It, therefore, always appears advisable when using experimental results in kinetic models, to take possible errors of up to one order of magnitude into account for the relaxation times. At temperatures of up to 1000 K, experience has shown that the experimental results scatter by a factor of two.

2.4. Interferences of the Boltzmann Distribution

With the help of Equation (2.3.-1), one can describe the change in the distribution density of the various energy levels of a vibrational degree of freedom as a result of VT-collisions. Now, an examination will be conducted into how the transition between two states 0 and 1 takes place, when the distribution densities of both states can be described by Boltzmann distributions which correspond to the kinetic gas temperatures T_0 and T_1 . From Equation (2.3.-1) to (2.3.-3), one obtains, with the abbreviation $y_1 = \exp(-\theta/T_1)$, this relationship

$$\dot{x}_n = \alpha \cdot \{n \cdot y_1 \cdot x_{n-1} - [n + (n+1) \cdot y_1] \cdot x_n + (n+1) \cdot x_{n+1}\} \quad .$$

Based on the assumption, that the solution is a Boltzmann distribution function which corresponds to a temperature T between T_0 and T_1 , therefore, the equation

$$x_n(t) = (1-y) \cdot y^n$$

is set up with $y = y(t)$. By insertion into the equation system, one obtains for y the differential equation

$$\dot{y} = \alpha \cdot (1-y) \cdot (y_1 - y) \quad .$$

This equation is now independent of n . It means that during the entire change in state, there is a Boltzmann distribution. Under consideration of the limiting conditions

$$y(t=0) = y_0 \quad ,$$

$$y(t \rightarrow \infty) = y_1$$

the solution of the differential equation becomes

$$y = \frac{(y_0 - 1) \cdot y_1 - (y_0 - y_1) \cdot e^{-\alpha(1-y_1) \cdot t}}{(y_0 - 1) - (y_0 - y_1) \cdot e^{-\alpha(1-y_1) \cdot t}}$$

The effect of an additional excitation from VV-collisions will now be examined. Let the test gas consist of a mixture of two gases, with one effective vibrational degree of freedom for each gas. The changes in the distribution densities on account of VT-collisions are then given by

$$\dot{x}_n = (\alpha_x \cdot A + \alpha_y \cdot B) \cdot \{n \cdot \phi_x(T_1) \cdot x_{n-1} - [n + (n+1) \cdot \phi_x(T_1)] \cdot x_n + (n+1) \cdot x_{n+1}\}$$

and

$$\dot{y}_n = (\beta_x \cdot A + \beta_y \cdot B) \cdot \{n \cdot \phi_y(T_1) \cdot y_{n-1} - [n + (n+1) \cdot \phi_y(T_1)] \cdot y_n + (n+1) \cdot y_{n+1}\}$$

y_n now stands for the distribution density of the admixed gas, and the Boltzmann factors are given by $\phi_i(T_j)$. The designations A and B stand for the mole fractions of the two gases in the mixture. The reaction velocity constants are described by α_i and β_i , where i stands for the collision partner. In addition, the l^{th} level of the oscillator x and the m^{th} level of the oscillator y are to exercise an influence against each other. In addition to the changes in distribution densities on account of VT-collisions, a distribution density change, therefore, takes place which becomes for the oscillator x

$$\dot{x}_1 = \gamma \cdot B \cdot (x_{1-1} \cdot y_m - x_1 \cdot y_{m-1})$$

Here, γ is the reaction velocity constant for this process. An expression for the solution

$$x_n = (1 - \phi_x) \cdot \phi_x^n$$

and

$$y_n = (1 - \phi_y) \cdot \phi_y^n$$

now only yields for $n \neq 1$ or for $n = m$ a differential equation for ϕ_x or ϕ_y , independent of n . For $n = 1$, one obtains for the oscillator x the following expression

$$\begin{aligned} \dot{\phi}_x = & (\alpha_x \cdot A + \alpha_y \cdot B) \cdot (1 - \phi_x) \cdot [\phi_x(T_1) - \phi_x] \\ & + \gamma \cdot B \cdot (1 - \phi_x) \cdot \phi_x^{l-1} \cdot (1 - \phi_y) \cdot \phi_y^{m-1} \cdot (\phi_y - \phi_x) \\ & / [1 \cdot \phi_x^{l-1} - (l+1) \cdot \phi_x^l] \end{aligned}$$

For this reason, one cannot get only one valid solution for each n , neither for ϕ_x nor for ϕ_y . This means that the Boltzmann distribution receives interference from the VV-collisions.

A closed solution of the differential equation system is not possible, and the extent of the interference can, therefore, not be determined without numerical methods. It is possible, however, to estimate when an interference from VV-collisions is substantial. Such is the case when the delivered energy cannot spread fast enough across all energy levels. Thus one obtains as the criterion for noticeable interferences

$$\dot{x}_{1VV} > \dot{x}_{1VT}$$

The lowest energy levels are the easiest to disturb because they have the greatest density. The case most advantageous for an interference, is $l = m = 1$. Thus the criterion now becomes much simpler

$$\left. \begin{aligned} \gamma \cdot B \cdot (x_0 \cdot y_1 - x_1 \cdot y_0) &> (\phi_x \cdot A + \alpha_y \cdot B) \\ &\cdot \{ \phi_x(T_1) \cdot x_0 - [1 + 2 \phi_x(T_1)] \cdot x_1 + 2 x_2 \} \end{aligned} \right\}$$

If a Boltzmann distribution prevails up to the noticeable introduction of the interference, then one obtains

$$\gamma > (\alpha_x \cdot \frac{A}{B} + \alpha_y) \cdot \frac{\phi_x(T_1) - [1 + 2\phi_x(T_1)] \cdot \phi_x + 2\phi_x^2}{(1 - \phi_y) \cdot \phi_y \cdot (\phi_y - \phi_x)}$$

An interference can take place only when $\phi_y - \phi_x > 0$. This, in turn, can only happen when the oscillator y is already substantially excited and, therefore, the expression

$$\alpha_x \cdot A + \alpha_y \cdot B \ll \beta_x \cdot A + \beta_y \cdot B \quad (2.4-1)$$

must be valid. Here again, the most advantageous case for an interference is $\phi_x \ll \phi_y$, so that one obtains

$$\gamma > (\alpha_x \cdot \frac{A}{B} + \alpha_y) \cdot \frac{\phi_x(T_1) - [1 + 2\phi_x(T_1)] \cdot \phi_x + 2\phi_x^2}{(1 - \phi_y) \cdot \phi_y}$$

Based on Equation (2.4-1), one must expect that ϕ_x is very small against $\phi_x(T_1)$ and against 1. A large denominator is also advantageous for the interference. The denominator for $\phi_y = 1/2$ becomes maximal so that one eventually obtains, as a (rough) estimate, the following expression

$$\gamma > (\alpha_x \cdot \frac{A}{B} + \alpha_y) \cdot 4 \cdot \phi_x(T_1) \quad (2.4-2)$$

Based on Equation (2.4-1), one must again expect that $\phi_x(T_1)$ is relatively large. The Boltzmann factor $\phi_x(T_1)$ cannot, however, exceed the numerical value of 1. As criterion, the following expression remains along with Equation (2.4-1)

$$\gamma > (\alpha_x \cdot \frac{A}{B} + \alpha_y) \cdot 4 \quad (2.4-3)$$

This condition, in no way, poses any unusual demands. In many cases, the reaction velocity constant of VV-reactions is higher than the constants of the also participating VT-reactions. There are, however, only very few cases where the validity of the Equation (2.4-1) is ensured. An accurate explanation for the extent of interferences can only be given by numerical calculation. One can, however, suspect a noticeable interference when conditions (2.4-1) and (2.4-3) are simultaneously fulfilled.

3. Application of the Model on CO₂-H₂O-N₂-O₂-He Mixtures.

In Chapter 2, the kinetic equations for the energy exchange in molecular gas mixtures were formulated in general terms so that an application for any given gas mixture is possible. Theory requires that for all gases of the mixture, the same number M of energy levels per vibrational degree of freedom be considered. Therefore, the number M orients itself in accordance with the highest necessary vibrational degrees of freedom. M can then be found with the help of the requirement that the energy content of the respective degree of freedom, up to a certain error, is equal to the same gas consisting of harmonic oscillators with M energy levels. This energy content is obtained by summation across all energy levels M as

$$e_{\text{vib}} = R \Theta \cdot \sum_{n=0}^M (n + 1/2) \cdot x_n \quad .$$

If the distribution densities can be described by a Boltzmann distribution, then one obtains

$$e_{\text{vib}} = R \Theta \cdot \frac{1 - \exp(-\Theta/T)}{1 - \exp[-(M+1) \cdot \Theta/T]} \cdot \sum_{n=0}^M (n + 1) \cdot \exp(-n \cdot \Theta/T) \quad .$$

After calculating the summation and after rearranging various expressions one obtains for the absolute vibrational energy

$$e_{\text{vib}} = R \Theta \cdot \left\{ \frac{1}{2} + \frac{\exp(-\Theta/T)}{1 - \exp(-\Theta/T)} - (M+1) \cdot \frac{\exp[-(M+1) \cdot \Theta/T]}{1 - \exp[-(M+1) \cdot \Theta/T]} \right\} \quad .$$

The finite number M of energy levels limits the maximum energy absorption to

$$e_{\text{vib}_{\text{max}}} = \lim_{T \rightarrow \infty} e_{\text{vib}} = 1/2 R \Theta \cdot (2M+1) \quad .$$

The vibrational energy stored in the molecule cannot exceed the dissociation energy D since, otherwise, the molecule falls apart. If one defines a characteristic dissociation temperature $\Theta_D = D/k$, where k is the Boltzmann constant, then with the characteristic vibrations Θ_j , the

following requirement is given by

$$\sum_{j=1}^J (n_j + 1/2) \cdot \theta_j \leq \theta_0 \quad (3.-1)$$

Here, J stands for the number of vibrational degrees of freedom of the respective gas. For such a gas, the portion of molecules in the vibrational ground state amounts to

$$x_{0,0,\dots,0} = \left[\sum_{n_1=0}^{N_1} \sum_{n_2=0}^{N_2} \dots \sum_{n_J=0}^{N_J} \exp \left(- \sum_{i=1}^J n_i \theta_i / T \right) \right]^{-1}$$

The summation limits N_i must always be chosen in such a way that Equation (3.-1) is satisfied. All of the stored vibrational energy in the gas is thus obtained with

$$e_{vib} = x_{0,0,\dots,0} \cdot R \cdot \sum_{i=1}^J \left\{ \theta_i \cdot \sum_{n_1=0}^{N_1} \sum_{n_2=0}^{N_2} \dots \sum_{n_J=0}^{N_J} \left[(n_i + 1/2) \cdot \exp \left(- \sum_{j=1}^J n_j \cdot \theta_j / T \right) \right] \right\}$$

Here again, the summation limits must be chosen so that Equation (3.-1) is valid. For molecules with only one vibrational degree of freedom, these calculations are simple. For three-atom molecules, however, there are already, in general, three vibrational degrees of freedom, with abnormalities not included. An n-fold abnormal degree of freedom must be treated like n normal degrees of freedom so that, for example, CO_2 has $J = 4$ degrees of freedom. In addition, one has to pay attention to the fact that with abnormal vibrational degrees of freedom, not all combinations of quantum numbers are possible. The selection rules for CO_2 are listed in Chapter 3.3. Calculations of the vibrational energy can then be carried out only with the help of simplified assumptions or in a numerical way. A possible simplification consists in the assumption that within the molecules, a continuous exchange of energy takes place which means that each degree of freedom can take up the same maximum energy content. For the various degrees of freedom one, therefore, obtains the number of energy levels to be considered as

$$M_j = \frac{\theta_0}{J \cdot \theta_j} - \frac{1}{2}$$

Fig. 3.-1 to 3.-3 show the vibrational energy content of CO₂, calculated in three different ways:

- Harmonic oscillator with indefinitely many energy levels.
- Harmonic oscillator with total energy limitation for all degrees of freedom.
- Harmonic oscillator with energy limitation for the individual degrees of freedom

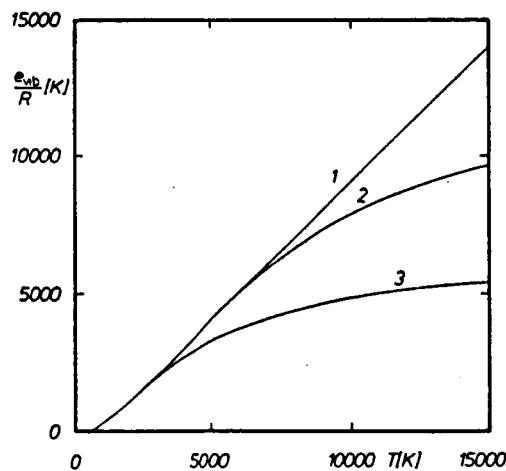


Fig. 3.-1

Plot of vibrational energy of the symmetrical valence oscillation for CO₂ versus the vibrational temperature.

- 1 : Harmonic oscillator with indefinitely many energy levels.
- 2 : Harmonic oscillator with limitation of total energy.
- 3 : Harmonic oscillator with limitation of energy for each vibrational degree of freedom.

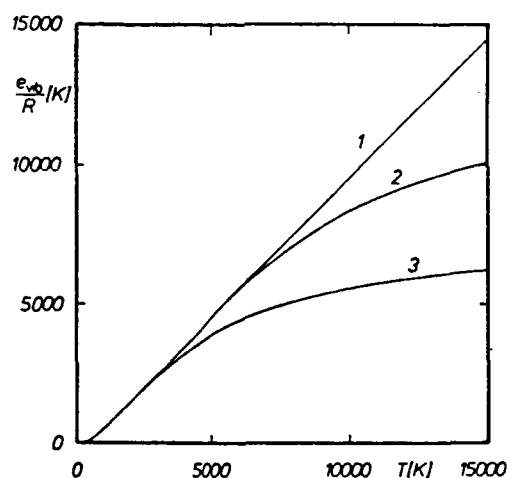


Fig. 3.-2

Plot of vibrational energy of the deformation oscillation for CO_2 versus the vibrational temperature.

- 1 : Harmonic oscillator with indefinitely many energy levels.
- 2 : Harmonic oscillator with limitation of total energy.
- 3 : Harmonic oscillator with limitation of energy for each vibrational degree of freedom.

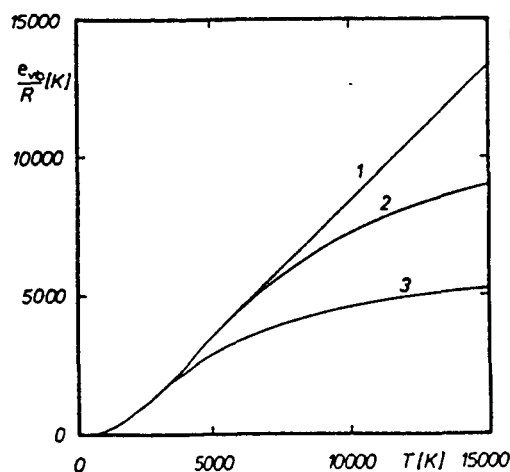


Fig. 3.-3

Plot of vibrational energy of the asymmetrical valence oscillation for CO_2 versus the vibrational temperature.

- 1 : Harmonic oscillator with indefinitely many energy levels.
- 2 : Harmonic oscillator with limitation of total energy.
- 3 : Harmonic oscillator with limitation of energy for each vibrational degree of freedom.

The question is now about the number of energy levels M_j which, when the simplified model is used, shows a lowest possible deviation compared to the model with total energy limitation. One finds for CO_2 at

temperatures of under 10000 K

for the bending oscillation

$$M_2 = 35 ,$$

for the symmetrical valence oscillation

$$M_1 = 18 ,$$

for the asymmetrical valence oscillation

$$M_3 = 10 .$$

Thus, there are at least 36 energy levels up for consideration in a kinetic model which contains CO_2 . For the system $\text{CO}_2 - \text{H}_2\text{O} - \text{N}_2 - \text{O}_2 - \text{He}$ at gas temperatures of under 10000 K, the conditions are given in Table 3.-1. For H_2O , only the bending oscillation was taken into account because the other two vibrational forms show very high characteristic temperatures. The consequence is that the predominant portion of the H_2O -molecules find themselves in the ground state of these vibrational forms.

	CO_2	H_2O	N_2	O_2
M_1	18	-	33	26
M_2	35	25	-	-
M_3	10	-	-	-

Table 3.-1

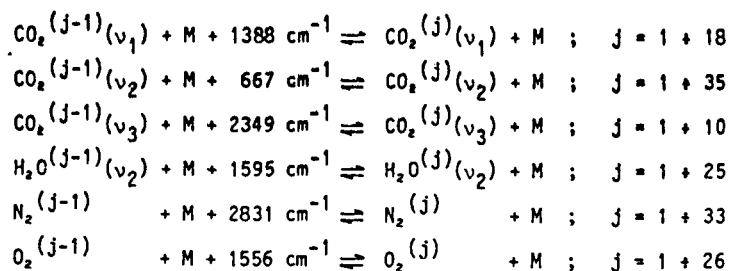
Number of energy levels to be considered.

The calculation of the reaction kinetics is done numerically. Due to the magnitude of the system, this can only be accomplished with the help of a computer. Programming of the general formulae which were developed in Chapter 2, is not always advantageous. The three-dimensional reaction matrices A_{VV} and A_V , for example, contain by necessity numerous zero elements. Also, when there are substantially differing values for the number M_j of energy levels of the degree of freedom j , then these general formulae don't necessarily offer an advantage. But this is not valid anymore when computers are available which can work more effectively at total vectorialization. The special formulation was preferred, however, since there was no vector computer available when the calculations for this paper were made. Therefore, only that number of energy levels listed in Table 3.-1 for each vibrational degree of freedom, was taken into account.

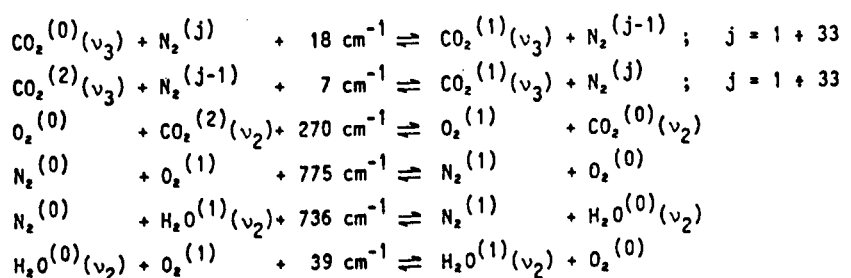
3.1 Reaction System and Numerical Treatment

The pertinent reactions were chosen, based on the tables by Taylor, Bitterman [6]. In the following scheme, the respective collision partner carries the designation M:

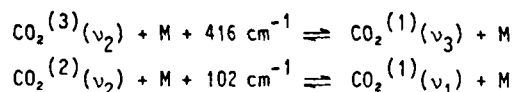
VT-Collisions: M = CO₂, H₂O, N₂, O₂, He



VV-Collisions (intermolecular):



VV-Collisions (intramolecular): M = CO₂, H₂O, N₂, O₂, He

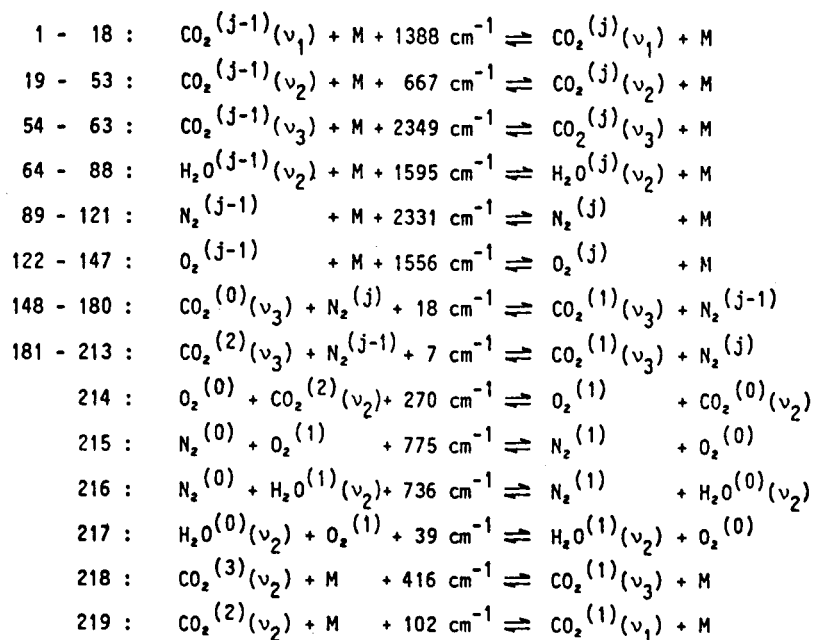


The last reaction is of special significance. It deals with the most important Fermi resonance reaction of the CO₂-molecule. One of the fastest and, therefore, also one of the most important reactions is the vibrational energy exchange between CO₂(ν_3) and N₂. Higher-excited

N_2 -molecules can participate in this process, according to Kleen, Mueller [18]. This applies mainly to all VV-reactions, but in this special case, a disturbance of the Boltzmann distribution is to be expected because of the high reaction velocity. Therefore, all nitrogen levels were included in both reactions which pertain to this energy exchange. Thus, the system at hand consists of 157 dependent variables which are designated as follows:

y(1)	ρ	Total density
y(2)	T	Gas temperature
y(3)	Δe_{vib}	Vibrational energy
y(4)	$\left. \begin{array}{l} \vdots \\ [CO_2^{(j)}(v_2)] \\ \vdots \\ [CO_2^{(j)}(v_2)] \\ \vdots \\ [CO_2^{(j)}(v_3)] \\ \vdots \\ [H_2O^{(j)}(v_2)] \\ \vdots \\ [N_2^{(j)}] \\ \vdots \\ [O_2^{(j)}] \end{array} \right\}$	Individual concentrations
\vdots		
y(22)		
y(23)		
\vdots		
y(58)		
y(59)		
\vdots		
y(69)		
y(70)		
\vdots		
y(95)		
y(96)		
\vdots		
y(129)		
y(130)		
\vdots		
y(156)		
y(157)	x	Path of particles

The reactions are counted as follows:



The heat effects of the individual reactions can be calculated from the intermediate wave numbers $\bar{\nu}$ according to

$$\Delta \epsilon = N_A \cdot h \cdot c \cdot \bar{\nu} = 11,964 \cdot \bar{\nu} \text{ J/mol}$$

In this equation, $\bar{\nu}$ must have the unit cm^{-1} .

For the individual reactions one obtains, therefore:

1 - 18 :	16 606	J/mol
19 - 53 :	7 980	J/mol
54 - 63 :	28 103	J/mol
64 - 88 :	19 083	J/mol
89 - 121 :	27 888	J/mol
122 - 147 :	18 616	J/mol
148 - 180 :	215	J/mol
181 - 213 :	78	J/mol
214 :	3 230	J/mol
215 :	9 272	J/mol
216 :	8 806	J/mol
217 :	467	J/mol
218 :	4 977	J/mol
219 :	1 220	J/mol

The system has six different vibrational degrees of freedom with the following characteristic temperatures:

CO ₂ (v ₁)	1998 K
(v ₂)	960 K
(v ₃)	3381 K
H ₂ O(v ₂)	2296 K
N ₂	3355 K
O ₂	2240 K

From the motion equations in Chapter 2.2. , one obtains

$$\dot{\rho} / \rho = \frac{R}{u^2 - R \cdot T} \cdot \dot{T} \quad ,$$

$$u = u_2 \cdot \rho_2 / \rho = \dot{y}(157) \quad ,$$

$$\dot{T} = \frac{1}{\frac{R u^2}{u^2 - R \cdot T} - R \cdot \frac{7}{2}} \cdot \dot{e}_{vib} ,$$

$$\dot{e}_{vib} = \sum \Delta \epsilon_i \cdot D_i + Q .$$

Q stands for the energy per volume, brought in from the outside. Such an energy supply is possible, for example, by the swelling, the sinking, or the action of a high-frequency excitation. According to Equation (2.2.-1), u is the momentary flow velocity, and Index 2 designates the initial state. From Chapter 2.1. it follows for all components that

$$\dot{c}_i = c_i \cdot \dot{p}/p + \sum D_j .$$

The second term on the right side takes the conversions in the individual reactions into account. The first term on the right side, on the other hand, stands for the concentration changes caused by state changes. The quotient \dot{p}/p will be abbreviated with a B in the following examination. Thus one obtains the following differential equations for each of the individual components:

$$\dot{y}(4) = B \cdot y(4) - D_1$$

$$\dot{y}(5) = B \cdot y(5) + D_1 - D_2 + D_{219}$$

$$\dot{y}(j) = B \cdot y(j) + D_{j-4} - D_{j-3} ; \quad j = 6, 7, \dots, 21$$

$$\dot{y}(22) = B \cdot y(22) + D_{18}$$

$$\dot{y}(23) = B \cdot y(23) - D_{19} + D_{214}$$

$$\dot{y}(24) = B \cdot y(24) + D_{19} - D_{20}$$

$$\dot{y}(25) = B \cdot y(25) + D_{20} - D_{21} - D_{214} - D_{219}$$

$$\dot{y}(26) = B \cdot y(26) + D_{21} - D_{22} - D_{218}$$

$$\dot{y}(j) = B \cdot y(j) + D_{j-5} - D_{j-4} ; \quad j = 27, 28, \dots, 57$$

$$\dot{y}(58) = B \cdot y(58) + D_{53}$$

$$\begin{aligned}
\hat{y}(59) &= B \cdot y(59) - D_{54} - \sum_{148}^{188} D_i \\
\hat{y}(60) &= B \cdot y(60) - D_{54} - D_{55} + \sum_{148}^{188} D_i + \sum_{181}^{213} D_i + D_{218} \\
\hat{y}(61) &= B \cdot y(61) + D_{55} - D_{56} - \sum_{181}^{213} D_i \\
\hat{y}(j) &= B \cdot y(j) + D_{j-6} - D_{j-5} ; \quad j = 62, 63, \dots, 68 \\
\hat{y}(69) &= B \cdot y(69) + D_{63} \\
\hat{y}(70) &= B \cdot y(70) - D_{64} + D_{216} - D_{217} \\
\hat{y}(71) &= B \cdot y(71) + D_{64} - D_{65} - D_{216} + D_{217} \\
\hat{y}(j) &= B \cdot y(j) + D_{j-7} - D_{j-6} ; \quad j = 72, 73, \dots, 94 \\
\hat{y}(95) &= B \cdot y(95) + D_{88} \\
\hat{y}(96) &= B \cdot y(96) - D_{89} + D_{148} - D_{181} - D_{215} - D_{216} \\
\hat{y}(97) &= B \cdot y(97) + D_{89} - D_{90} - D_{148} - D_{149} + D_{181} - D_{182} + D_{215} + D_{216} \\
\hat{y}(j) &= B \cdot y(j) + D_{j-8} - D_{j-7} - D_{j+51} + D_{j+52} + D_{j+84} - D_{j+85} ; \\
&\quad j = 98, 99, \dots, 128 \\
\hat{y}(129) &= B \cdot y(129) + D_{121} - D_{180} + D_{213} \\
\hat{y}(130) &= B \cdot y(130) - D_{122} - D_{214} + D_{215} + D_{217} \\
\hat{y}(131) &= B \cdot y(131) + D_{122} - D_{123} + D_{214} - D_{215} - D_{217} \\
\hat{y}(j) &= B \cdot y(j) + D_{j-9} - D_{j-8} ; \quad j = 132, 133, \dots, 155 \\
\hat{y}(156) &= B \cdot y(156) + D_{147}
\end{aligned}$$

For the conversion rates of each of the individual reactions one obtains:

$$D_i = \left(\sum_M \bar{k}_{j-M}^{C1} \cdot A_M \right) \cdot [CO_2^{(j-1)}(v_1)] - \left(\sum_M \bar{k}_{j-M}^{C1} \cdot A_M \right) \cdot [CO_2^{(j)}(v_1)]$$

$$i = 1 + 18$$

$$j = i$$

$$D_i = \left(\sum_M \bar{k}_{j-M}^{C2} \cdot A_M \right) \cdot [CO_2^{(j-1)}(v_2)] - \left(\sum_M \bar{k}_{j-M}^{C2} \cdot A_M \right) \cdot [CO_2^{(j)}(v_2)]$$

$$i = 19 + 53$$

$$j = i - 18$$

$$D_i = \left(\sum_M \bar{k}_{j-M}^{C3} \cdot A_M \right) \cdot [CO_2^{(j-1)}(v_3)] - \left(\sum_M \bar{k}_{j-M}^{C3} \cdot A_M \right) \cdot [CO_2^{(j)}(v_3)]$$

$$i = 54 + 63$$

$$j = i - 53$$

$$D_i = \left(\sum_M \bar{k}_{j-M}^{H2} \cdot A_M \right) \cdot [H_2O^{(j-1)}(v_2)] - \left(\sum_M \bar{k}_{j-M}^{H2} \cdot A_M \right) \cdot [H_2O^{(j)}(v_2)]$$

$$i = 64 + 88$$

$$j = i - 63$$

$$D_i = \left(\sum_M \bar{k}_{j-M}^N \cdot A_M \right) \cdot [N_2^{(j-1)}] - \left(\sum_M \bar{k}_{j-M}^N \cdot A_M \right) \cdot [N_2^{(j)}]$$

$$i = 89 + 121$$

$$j = i - 88$$

$$D_i = \left(\sum_M \bar{k}_{j-M}^O \cdot A_M \right) \cdot [O_2^{(j-1)}] - \left(\sum_M \bar{k}_{j-M}^O \cdot A_M \right) \cdot [O_2^{(j)}]$$

$$i = 122 + 147$$

$$j = i - 121$$

$$D_i = \bar{k}_1^{C3-N} \cdot [CO_2^{(0)}(v_3)] \cdot [N_2^{(j)}] - \bar{k}_1^{C3-N} \cdot [CO_2^{(1)}(v_3)] \cdot [N_2^{(j-1)}]$$

$$i = 148 + 180$$

$$j = i - 147$$

$$D_i = \vec{k}_2^{C3-N} \cdot [CO_2^{(2)}(v_3)] \cdot [N_2^{(j-1)}] - \vec{k}_2^{C3-N} \cdot [CO_2^{(1)}(v_3)] \cdot [N_2^{(j)}]$$

$$i = 181 + 213$$

$$j = i - 180$$

$$D_{214} = \vec{k}^{O-C2} \cdot [O_2^{(0)}] \cdot [CO_2^{(2)}(v_2)] - \vec{k}^{O-C2} \cdot [O_2^{(1)}] \cdot [CO_2^{(0)}(v_2)]$$

$$D_{215} = \vec{k}^{N-O} \cdot [N_2^{(0)}] \cdot [O_2^{(1)}] - \vec{k}^{N-O} \cdot [N_2^{(1)}] \cdot [O_2^{(0)}]$$

$$D_{216} = \vec{k}^{N-H2} \cdot [N_2^{(0)}] \cdot [H_2O^{(1)}(v_2)] - \vec{k}^{N-H2} \cdot [N_2^{(1)}] \cdot [H_2O^{(0)}(v_2)]$$

$$D_{217} = \vec{k}^{H2-O} \cdot [H_2O^{(0)}(v_2)] \cdot [O_2^{(1)}] - \vec{k}^{H2-O} \cdot [H_2O^{(1)}(v_2)] \cdot [O_2^{(0)}]$$

$$D_{218} = (\sum_M \vec{k}_M^{C2-C3} \cdot A_M) \cdot [CO_2^{(3)}(v_2)] - (\sum_M \vec{k}_M^{C2-C3} \cdot A_M) \cdot [CO_2^{(1)}(v_3)]$$

$$D_{219} = (\sum_M \vec{k}_M^{C1-C2} \cdot A_M) \cdot [CO_2^{(2)}(v_2)] - (\sum_M \vec{k}_M^{C1-C2} \cdot A_M) \cdot [CO_2^{(1)}(v_1)]$$

A_M denotes the momentary concentration of gas type M . The indexing of the reaction velocity constant k

at $\vec{k}, \overleftarrow{k}$ refers to the direction of the reaction,
and
at k^{a-b} refers to the participating degrees of freedom.

The degrees of freedom are designated with the abbreviations

C1 for $CO_2(v_1)$,

C2 for $CO_2(v_2)$,

C3 for $CO_2(v_3)$,

H2 for $H_2O(v_2)$,

N for N_2 ,

O for O_2 .

The indexing of the reaction velocity constants at k_{j-M} refers to the participating end level j at VT-reactions and the collision partner M

who evolves unchanged from the reaction involving VT-reactions. An exception is made by the reactions of the VV-interaction between C3 and N. There

k_1^{C3-N} designates the reaction with the heat effect 18 cm^{-1} , and

k_2^{C3-N} designates the reaction with the heat effect 7 cm^{-1} .

With respect to the electrical excitation of the vibrational degrees of freedom, the reader is referred to Chapter 3.2. and Appendix B.

The solution of the described system of differential equations is performed numerically with the help of the Runge-Kutta Method. A control for the interval was built into the computer program, so that the relative accuracy with which each time interval is calculated, always remains within the limits (10^{-5} , 10^{-7}). Numerical difficulties occurred only at those locations where the electrical excitation of the vibrational degrees of freedom ceased, or where the effect of radiation fields begins or ends. There, the interval control can fail when these locations are situated between two time intervals. The interval control then swings back and forth between decrease and increase of the interval. This deficiency could be remedied in that the interval control at these locations was blocked whenever necessary, enabling the calculation past these locations by using the smaller interval. Thereafter, the blockage was lifted again. In this way, a satisfactory calculation accuracy is always assured.

3.2. Overview Over the Kinetic Data

In Chapter 2.3.1., it was demonstrated how one can produce reaction velocity constants for the individual energy exchange reactions when the relaxation time or the median transition probability is given. For VT-reactions, one would, therefore, expect a temperature dependence in the form of

$$\bar{k} = A \cdot \sqrt{T} \cdot \exp(-B \cdot T^{-1/3})$$

Experience shows, however, that in this form there is no satisfactory fit to the experimental results. For VT-reactions, therefore, Blauer, Nickerson [7] propose the form

$$\ln \bar{k} = A + B \cdot T^{-1/3} + C \cdot (T^{-1/3})^2 \quad (3.2.-1)$$

It is evident that with this expression a satisfactory fit to all experimental results for VT-reactions is possible. The coefficients A, B, and C, proposed by Blauer, Nickerson were not used, however, because they were developed mainly with the aid of purely theoretical data by Herzfeld [17], and these data do not show good agreement with more up-to-date measurements. Instead, those coefficients were used which had been developed with the help of an interactive, graphical computer program by means of the fit of Equation (3.2.-2.) to experimental results. These coefficients are listed in Appendix A. For some VT-reactions there are only very few experimental results available; or only those experimental results are available for some of the possible collision partners with respect to the model at hand. In these cases it was possible apply the systematic approach by Millikan, White [8]. They give as the general formula for the relaxation time of VT-reactions

$$\ln (\tau_{\text{vib}} \cdot p [\text{sec} \cdot \text{atm}]) = 1,16 \cdot 10^{-3} \cdot \sqrt{\mu} \cdot \Theta^{4/3} \cdot (T^{-1/3} - 0,015 \cdot \mu^{1/4}) - 18,42 \quad (3.2.-2)$$

where μ stands for the reduced collision mass and Θ for the characteristic vibrational temperature of the excited collision partner. This theory was tested by my own investigations where it was determined that the constant with the value of 18.42 wasn't valid for all reactions. One can list for each reaction its own constant so that the differing results for various collisions partners can be reproduced with sufficient accuracy by Equation (3.2.-2). This method was also applied to the velocity constants for the Fermi-resonance. For this reaction, only very few experimental results are available; but they fit very well into the systematic approach. Equation (3.2.-2) can be reduced to the general form

$$\ln (\tau_{\text{vib}} \cdot p) = A^* + B^* \cdot T^{-1/3}$$

From it, we obtain for the reaction velocity constant in accordance with Equation (3.2.-2)

$$\ln \bar{k} = A + \ln \left[\frac{T}{1 - \exp(-\Theta/T)} \right] - B \cdot T^{-1/3} \quad .$$

The coefficients for the VT- and the V-reactions which were developed with the help of the systematic approach by Millikan, White [8], are also listed in the appendix. In the remaining cases, where there were neither experimental results available nor help from the systematic approach by Millikan, White [8], the velocity constants were determined with the aid of theoretical calculations. Using known experimental data, some of the familiar theories from literature were checked for their suitability. These were the Schwartz-Slowsky-Herzfeld Theory [23], and the theories by Herzfeld, Litovitz [22], Nikitin [24], and Widom [14]. The best reproduction of the experimental results was achieved with the theory of Widom [14]. The velocity constants, determined with this theory, were subjected to the same procedure as the experimental results and produced in the form of Equation (3.2.-1). Coefficients A, B, and C, thus developed, are also listed in the appendix. The temperature dependence of the reaction velocity constants for VV-reactions varies widely. According to Taylor, Bitterman [6], one generally obtains

$$\bar{k} \sim \sqrt{T} \cdot P(T) \quad ,$$

where the temperature dependence of the transition probability P can show differing tendencies. Generally, however, one can expect that the median transition probability with VV-reactions depends less upon the gas temperature than is the case with VT-reactions. For VV-reactions in this paper, the expression

$$\ln \bar{k} = A + B \cdot \sqrt{T} + C \cdot (\sqrt{T})^2 \quad (3.2.-3)$$

is given. The experimental results can be satisfactorily described with the aid of Equation (3.2.-3). Coefficients A, B, and C which were also determined by using a graphical match process, are listed in Appendix A, just like the other constants for the VT-reactions. The V-reaction between the vibrational states $\text{CO}_2^{(3)}(\nu_2)$ and $\text{CO}_2^{(1)}(\nu_3)$ was treated in the same way as the VT-reactions. The reaction velocity constants of the VT-reactions stand for the reactions between the vibrational ground state

and the first excited vibrational state. With the help of Equation (2.3.-2) and because of $k \sim P$ (median transition probability) one can calculate all other reaction velocity constants.

3.3. Small Signal Amplification

In a formal way, small signal amplification is nothing else than the negative absorption coefficient: if a radiation field is superimposed over a flowing gas mixture, and if the absorption coefficient for this radiation field becomes negative because of an inversion, then the radiation field is intensified by the passing of the gas. A prerequisite for the observation of the small signal amplification is that the radiation field is sufficiently weak so that the population densities of the participating energy levels are not significantly changed, and that no significant amount of energy is pulled away from the gas mixture by radiation. The small signal amplification is an important quantity which permits an evaluation of maximum laser efficiency which can be withdrawn from the gas mixture. The small signal amplification is given by

$$g = \frac{\lambda_{jk}^2 \cdot a_{jk}}{8\pi} \cdot f(\nu, \nu_{jk}) \cdot (n_j - n_k \cdot \frac{g_j}{g_k})$$

λ_{jk} stands for the wave length of the radiation transition $j \rightarrow k$, a_{jk} stands for the spectral probability of spontaneous emission, and $f(\nu, \nu_{jk})$ stands for the line form function. Quantities $n_{j,k}$ and $g_{j,k}$ stand for the population density and the weights of the upper and lower laser levels.

The line form function is subject to three influences:

- Natural line width which is created by the statistical distribution of the optical transition probability. The natural line width does not depend on pressure and temperature.
- Doppler broadening which is created by the presence of a molecular velocity spectrum. The Doppler broadening of a line is proportional to \sqrt{T} .

- Collision- or pressure broadening which is a consequence of the statistical distribution of the molecular collision frequency. The pressure broadening of a line is proportional to p/\sqrt{T} .

For the 10.6μ - laser line of CO_2 (transition $00^*1 \rightarrow 10^*0$), the following values result:

Natural line width	$\Delta \nu_N = 67 \text{ Hz}$,
Doppler width (300 K, 45 mbar)	$\Delta \nu_D = 58 \text{ MHz}$,
Pressure width (300 K, 45 mbar)	$\Delta \nu_p = 323 \text{ MHz}$.

Under laser conditions there are going to be smaller values for the line width. This is not, however, within the scope of this paper. At ambient temperatures and at higher temperatures, the natural line width is always negligible compared to the two other influences. In thinned gases, the pressure broadening is often small compared to the Doppler broadening, but depending on temperature, it can also reach the same magnitude. If one takes into account only the Doppler broadening when determining the line form, then the error isn't large even in the latter case, because the line form in the vicinity of the middle of the line is primarily determined by the Doppler broadening. The line form function at the middle of the line is then

$$f(\nu_{jk}) = \lambda_{jk} / \sqrt{2\pi RT}$$

In the following, the term "small signal amplification" is meant to mean the small signal amplification in the center of a pure, Doppler-broadened spectral line. Weight g_j of an energy level j is the number of solutions of the Schrodinger equation which exist for the corresponding energy amount; it, therefore, corresponds at the same time to the degree of degeneration. The CO_2 -molecule has three vibrational degrees of freedom, one of which, namely the bending vibration, exhibits a twofold degeneration. Each given vibrational state can, therefore, be described by four quantum numbers which are expressed by

$$\nu_1 \nu_2^1 \nu_3$$

where 1 stands for the quantum number of the angular momentum which is tied to the quantum number ν_2 by the rule

$$v_2 \text{ even} \rightarrow l = v_2, v_2-2, \dots, 0$$

$$v_2 \text{ odd} \rightarrow l = v_2, v_2-2, \dots, 1$$

All vibrational states with $l = 0$, therefore, have the weight of 1 and all vibrational states with $l > 0$ have the weight of 2. The simplest selection rules for optically permissible vibrational transitions are

$$\Delta v_2 - \text{even}, \Delta l = 0, \Delta v_3 \text{ odd}$$

$$\Delta v_2 - \text{odd}, \Delta l = 1, \Delta v_3 \text{ even}.$$

Aside from this, there is a multitude of other optically permissible transitions. All transitions, however, lie in the medium to the far infrared region. Pure vibrational transitions are seldom observed. With most spectral lines, one deals with rotational vibration transitions. Not only does the vibrational state of the molecule change, but also its rotational state. Differentiations are made among P-, Q-, and R-transitions where the corresponding letters are followed by the rotational quantum number which would enter itself for the molecule after the emission of a light quantum. The letters stand for the following changes in state:

$$J \text{ even } \Delta J = +1 \text{ P - Branch,}$$

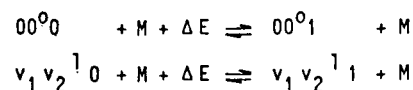
$$J \text{ either } \Delta J = 0 \text{ Q - Branch,}$$

$$J \text{ even } \Delta J = -1 \text{ R - Branch.}$$

The occupation density distribution of rotational degrees of freedom has a maximum J_{\max} for certain rotational quantum numbers. This depends on the rotational temperature (which for the model at hand is assumed to be equal to the translational temperature), when it is a matter of equilibrium distribution. This is also assumed for the model at hand. At room temperature, the transitions of the strongest intensities for the CO_2 -molecule lie at P20 and R20. This corresponds to transitions with $J = 19 \rightarrow 20$ and $J = 21 \rightarrow 20$.

The rate equations for the reaction system were determined under the assumptions that the vibrational degrees of freedom of the CO_2 -molecule influence one another only through reactions of the second order and that the reaction velocity constants for the levels of a vibrational degree of freedom do not depend on the vibrational states of other vibrational degrees of freedom.

In this sense, for example, the reactions



are equivalent. The population density of a given level is then given by the expression

$$n_j = n \cdot \psi(\nu_1) \cdot \psi(\nu_2) \cdot \psi(\nu_2' = 1) \cdot \psi(\nu_3)$$

n stands for the particle density of CO_2 , and $\psi(x)$ stands for the probability that a CO_2 -molecule finds itself in the vibrational state x . For state 03^10 , one obtains the population density

$$n_j = n \cdot \psi(00^00, \nu_1) \cdot \psi(03^00) \cdot \psi(01^00) \cdot \psi(00^00, \nu_3)$$

The state $0\nu_2^00$ for odd ν_2 is not real, it presents only formal help.

3.4. Effect of Superimposed Radiation Fields

Now the effect of an approximately resonant radiation field will be considered which acts perpendicular to the direction of flow. Let this field have the spectral radiation density L_ν^* on one spectral line ν_{jk} . Between the participating energy levels, the energy flow

$$\dot{E}/V = g \cdot L_\nu$$

is thus created. After dividing by the molecular energy difference between the energy levels, one obtains the concentration change of the vibrational levels for

$$\dot{c} = \pm g \cdot L_\nu / \Delta E_{jk}$$

* This designation corresponds to DIN 5496 "Temperature Radiation"; instead many papers generally use the designation "Intensity" and the formula symbol I_ν .

The positive sign is meant for the lower level which becomes more populated by the transition; and the negative sign stands for the upper level which becomes emptied. The energy difference between the two levels is obtained from

$$\Delta E_{jk} = h \cdot \nu_{jk} \cdot N_A$$

where $N_A = 6.023 \times 10^{23} \text{ mol}^{-1}$ is Avogadro's constant. Finally, the energy flow due to radiation must be given consideration in the equation for vibrational energy because the emitted light quanta generally depart from the flow.

With this kinetic model for the vibrational energy exchange in flowing gas mixtures which contain CO_2 , H_2O , N_2 , O_2 , and He, it is possible to investigate a multitude of processes. They include heating and cooling processes, excitation by high frequency, relaxation processes after gas-dynamic collisions and gas-dynamic CO_2 -lasers. In the following chapter, the presented model will be applied to some examples.

4. Applications

With the help of the kinetic model for the CO_2 , H_2O , N_2 , O_2 , and He mixture, it is possible to investigate radiation transitions of the CO_2 -molecule for their potential laser fitness. The model will, first of all, be checked with the help of known data for a cross-current CO_2 -laser with HF-impulse. Then, additional laser transitions, activated by various pump methods, will be investigated.

4.1. Calculation of a Cross-Current CO_2 -Laser with HF-Impulse

The subject of this chapter is the testing of the developed model using the data for a cross-current CO_2 -laser with high-frequency impulse. For this case, there are various experimental results available in literature. An accurate description of such a laser can be found in Jacoby [9]. With the help of Fig. 4.1.-1, the operational principle will be explained. A CO_2 - N_2 - He mixture in the ratio of $\text{CO}_2:\text{N}_2:\text{He} = 0.044 : 0.186 : 0.77$ flows through

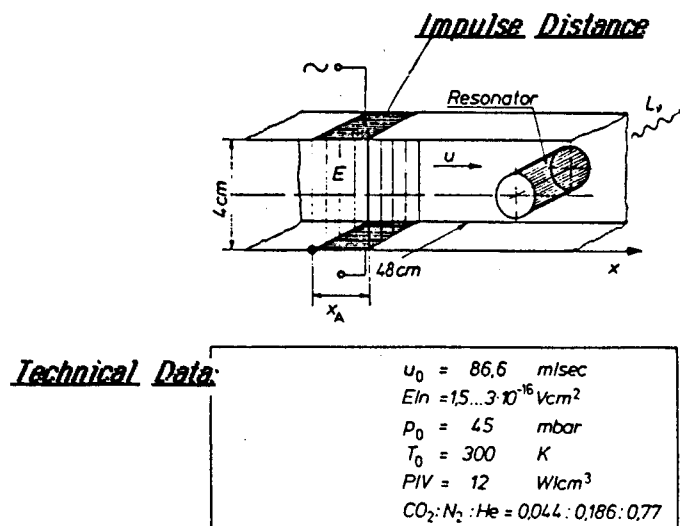


Fig. 4.1.-1

Schematics and technical data for a cross-current CO_2 -laser with high-frequency impulse, according to Jacoby [9].

a rectangular channel of constant diameter, and passes, first of all, through an impulse distance where the vibrational degrees of freedom of CO_2 and N_2 are subjected to energy in form of electromagnetic high-frequency radiation. The flow carries the HF-discharge downstream. In the model, this process is taken into account by assuming a discharge current density passage across the path of flow. Armandillo, Kaye [10] propose the passage which is given by

$$j(x) = j_0 \cdot \pi \cdot \frac{x}{x_A} \cdot \sin\left(\pi \cdot \frac{x}{x_A}\right)$$

j_0 stands for the median current density in the region of the impulse which stretches along path x_A . Fig. 4.1.-2 shows the dependence of this

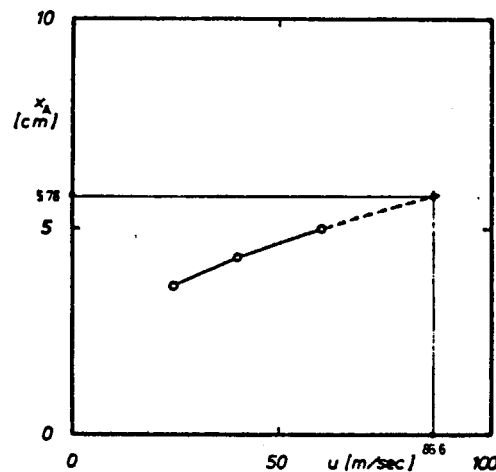


Fig. 4.1.-2

Dragging of the impulse distance by the current, according to Armandillo, Kaye [10].

distance x_A on the current velocity. In the case at hand, one obtains by extrapolation an impulse distance $x_A = 6$ cm in length. In the electrical field of the impulse distance some electrons which happen to be there, are

accelerated and liberate additional electrons through collisions with gas particles. If field strength E is suitably chosen, then the collisions with electrons result in an excitation of the vibrational degrees of freedom. For this process, the Boltzmann equation was solved by Nighan [11]. The results can be found in the form of excitation coefficients for the individual vibrational degrees of freedom. These calculations as well as the experimental results by Novgorodov, et alii [25] show that the velocity spectrum of the electrons under these conditions can no longer be described with the help of a Maxwell distribution.

With the help of a simple approximation, one obtains the excitation coefficients even without the Boltzmann equation. For this it is assumed that the velocity spectra of the electrons parallel and perpendicular to the field lines can be described by differing Maxwell distributions. These calculations are carried out in Appendix B. The excitation coefficients thus gained, agree well with the results by Nighan. As a result of the HF-impulse, a crowding of the vibrational state 00^*1 of CO_2 comes about compared to the states 10^*0 and 02^*0 , which makes the liberation of electromagnetic radiation with the help of a resonator possible. With the help of the model at hand, Fig. 4.1.-3 shows the calculated passage of the small signal amplification along the path of flow for the radiation transition $00^*1 \rightarrow 10^*0$. The wave length $\lambda = 10.5915 \mu\text{m}$ belongs to this transition P 20. The calculations agree well with the measurements published by Jacoby [9]. Figs. 4.1.-4 to 4.1.-7 show that, in this case, all participating vibrational degrees of freedom display disturbances in the Boltzmann distribution. This is attributed mainly to the high-frequency impulse.

The relationship (2.3.-2) is no longer valid for the transition probability due to electron collisions. The excitation rates due to high-frequency impulse are, moreover, substantially larger than the transfer rates through collisions with other gas particles, so that certain vibrational energy levels were given preferred excitation. To a smaller extent, the disturbances in the Boltzmann distribution are caused by the influence of VV-reactions. The disturbance of the Boltzmann distributions of the laser levels is of special significance. Without the strong disturbances of the asymmetrical valence modes of CO_2 , a substantially lower small signal amplification would have been expected.

- Experiment according to Jacoby [9]

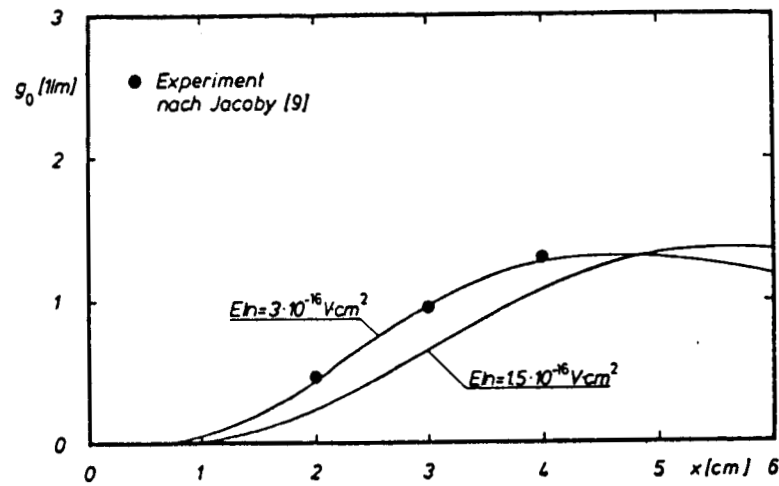


Fig. 4.1.-3

Trace of small signal amplification in a cross-current CO_2 -laser according to Jacoby [9] for the crossing $00^*1 \rightarrow 10^*0$, P20 with a wavelength of $10.5915 \mu\text{m}$.

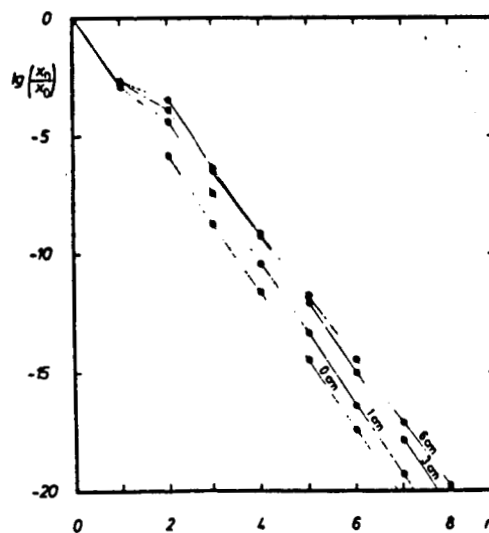


Fig. 4.1.-4

Trace of of the occupation density distribution in the cross-current CO_2 -laser according to Jacoby [9] for the symmetrical valence oscillation of CO_2 without the effect of a radiation field.

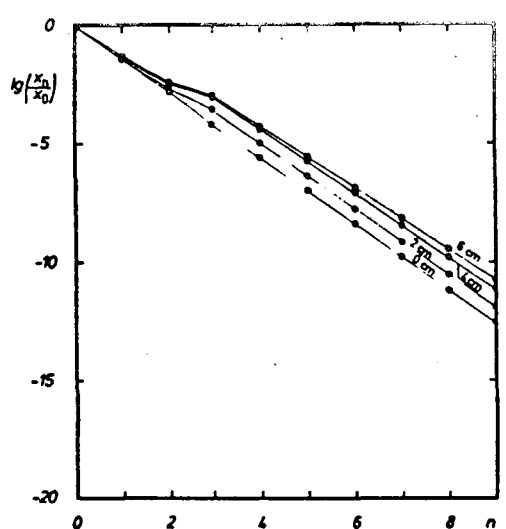


Fig. 4.1.-5

Trace of the occupation distribution density in the cross-current CO_2 -laser according to Jacoby [9] for the deformation oscillation of CO_2 without the effect of a radiation field.

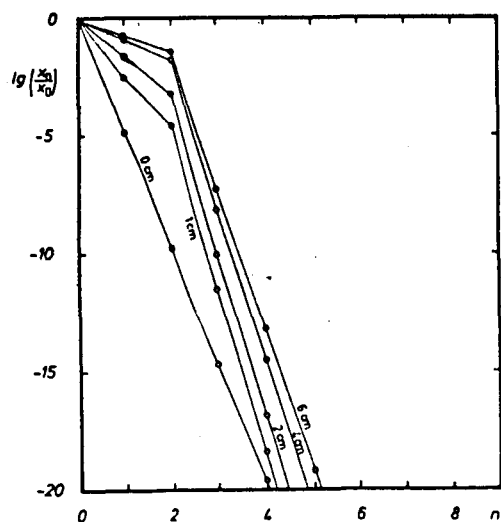


Fig. 4.1.-6

Trace of the occupation density distribution in the cross-current CO_2 -laser according to Jacoby [9] for the asymmetrical valence oscillation of CO_2 without the effect of a radiation field.

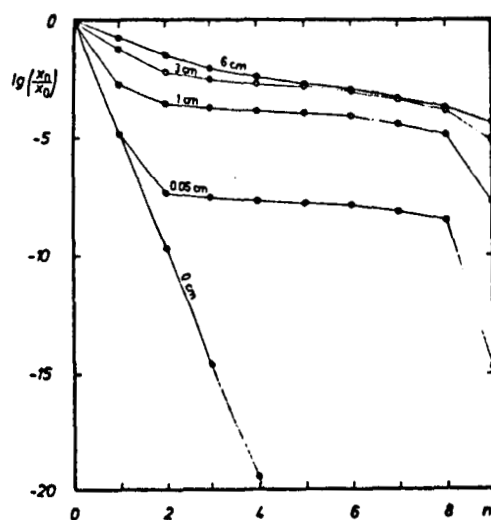


Fig. 4.1.-7

Trace of the occupation density distribution in the cross-current CO_2 -laser according to Jacoby [9] for nitrogen without the effect of a radiation field.

4.2. Examination of Additional CO₂-Laser Crossings

With the help of electrical discharges, one can easily activate the CO₂-laser crossings $00^*1 \rightarrow 10^*0$ at 10.6 μm , and $00^*1 \rightarrow 02^*0$ at 9.6 μm in CO₂-containing gas mixtures. Given by the level position, one can expect a maximum efficiency of about 40%. For this reason, CO₂-laser systems have gained substantial importance, among other fields, in the processing of materials. Because of level position and selection rules for radiation crossings, one can imagine lasers with much higher efficiencies. We are talking about lasers with crossings of $02^*0 \rightarrow 01^10$ at 16 μm and $10^*0 \rightarrow 01^10$ at 14 μm . In addition, the 16 μm -laser is of special importance. In this case, there is the possibility to radiate UF₆ in an isotope-selective manner and thus separate the isotope. A method for the generation of the necessary 16 μm -radiation was proposed by Wexler, et alii [12]. In this method, the inverted medium is discharged above the 9.6 μm -line. Thus the upper laser level is populated for the 16 μm -crossing so that one can expect an inversion. With the help of the model at hand, we shall now examine whether or not this expectation becomes fulfilled. The laser described in the previous section, will now be utilized as the 9.6 μm -laser. With this laser, one can reach a radiation field with an intensity of at least 600 W/cm² at the 9.6 μm -crossing. Calculations with the model at hand show that the necessary prerequisites for the 16 μm -crossing can, indeed, be attained in this manner. Fig. 4.2.-1 shows the trace of the amplification for the 9.6 μm -line and the trace of the small signal amplification for the 16 μm -line. This calculation assumed that the 9.6 μm -laser beam has an expansion of 2 cm in the direction of flow, and that the corresponding resonator is placed in the vicinity of maximum small signal amplification. Fig. 4.2.-2 to 4.2.-5 show the traces of the occupation density distribution of the individual vibrational degrees of freedom in the effective zone of the radiation field. Fig. 4.2.-3 shows that there is, on account of the radiation field, an almost undisturbed Boltzmann distribution for the deformation oscillation ν_2 . A similar calculation was carried out for the examination of the 14 μm -crossing. In this case, the flow medium was discharged above the 10.6 μm crossing, thus populating level 10^*0 . Fig. 4.2.-6 shows that in this manner, a very high small signal amplification for the 14 μm -line is obtained.

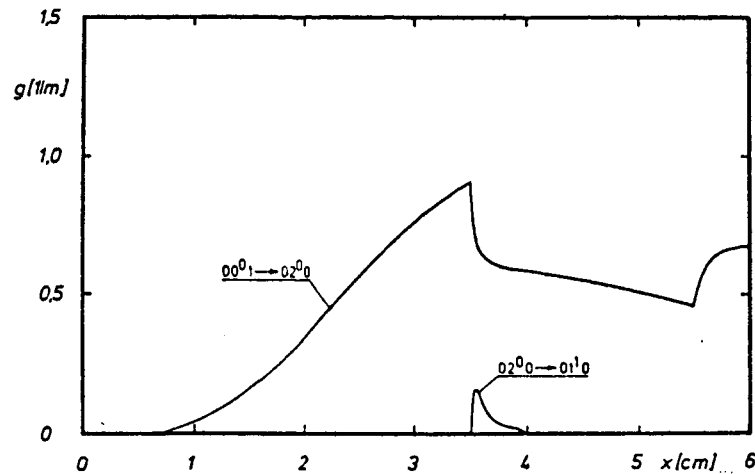


Fig. 4.2.-1

Signal amplification for the crossing $00^0_1 \rightarrow 02^0_0$, P20 with $\lambda = 9.5525 \mu\text{m}$ at a spectral radiation density of 600 W/cm^2 and a small signal amplification for the crossing $02^0_0 \rightarrow 01^1_0$, P20 with $\lambda = 16.1601 \mu\text{m}$ in the CO_2 -laser according to Jacoby [9].

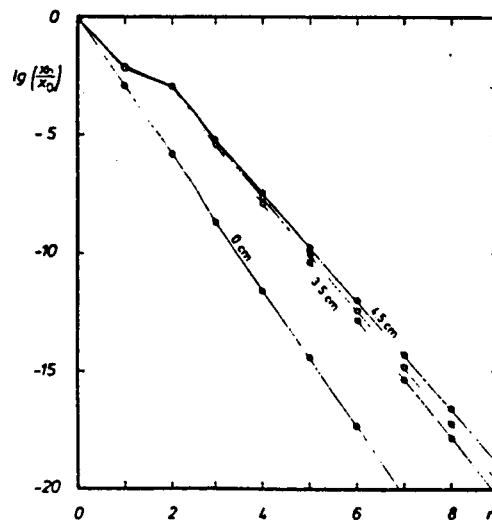


Fig. 4.2.-2

Trace of the occupation density distribution in the cross-current CO_2 -laser according to Jacoby [9] for the symmetrical valence oscillation of CO_2 at a spectral density of 600 W/cm^2 with $\lambda = 9.5525 \mu\text{m}$.

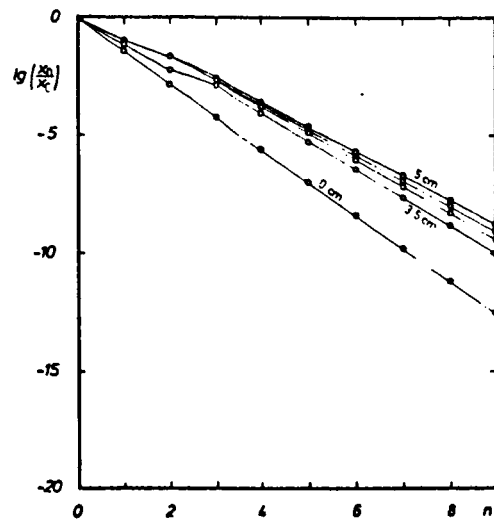


Fig. 4.2.-3

Trace of the occupation density distribution in the cross-current CO_2 -laser according to Jacoby [9] for the deformation oscillation of CO_2 at a spectral density of 600 W/cm^2 with $\lambda = 9.5525 \mu\text{m}$.

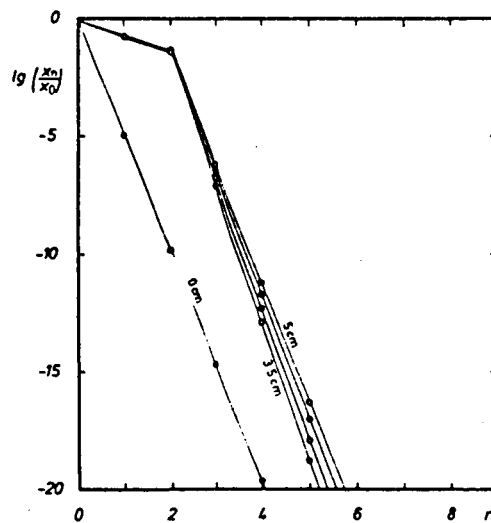


Fig.4.2.-4

Trace of the occupation density distribution in the cross-current CO_2 -laser according to Jacoby [9] for the asymmetrical valence oscillation of CO_2 at a spectral density of 600 W/cm^2 with $\lambda = 9.5525 \mu\text{m}$.

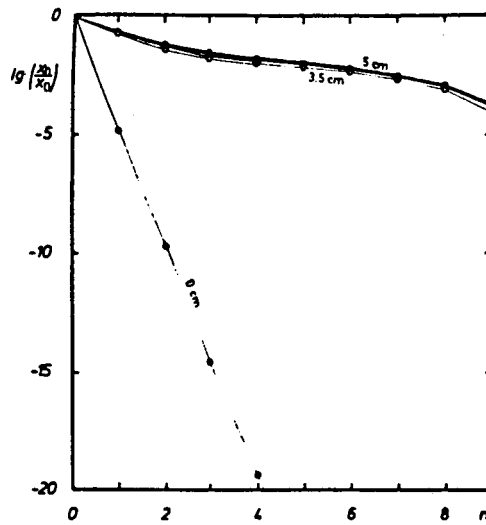


Fig. 4.2-5

Trace of the occupation density distribution in the cross-current CO_2 -laser according to Jacoby [9] for nitrogen at a spectral density of 600 W/cm^2 with $\lambda = 9.5525 \mu\text{m}$.

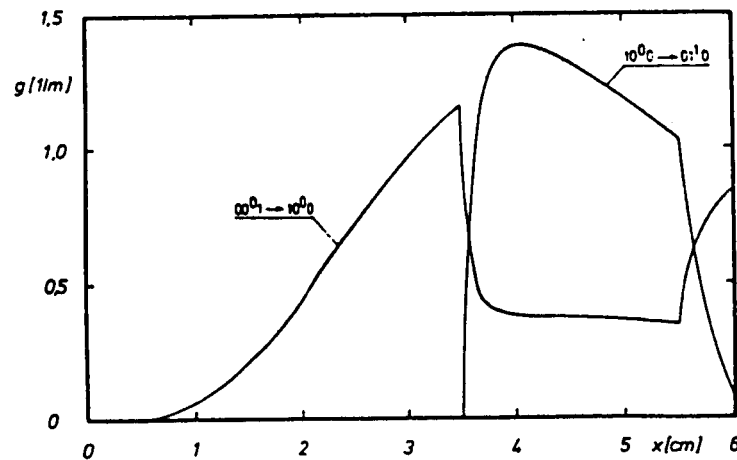


Fig. 4.2-6

Signal amplification for the crossing $00^*1 \rightarrow 10^*0$, P20 with $\lambda = 10.5915 \mu\text{m}$ at a spectral radiation density of 600 W/cm^2 and small signal amplification for the crossing $10^*0 \rightarrow 01^*1$, P20 with $\lambda = 13.8730 \mu\text{m}$ in the CO_2 -laser according to Jacoby [9].

Trace of the occupation density distribution in a cross-current CO₂-laser according to Jacoby [9] for the symmetrical valence oscillation of CO₂ at a spectral radiation density of 600 W/cm² with $\lambda = 10.5915 \mu\text{m}$.

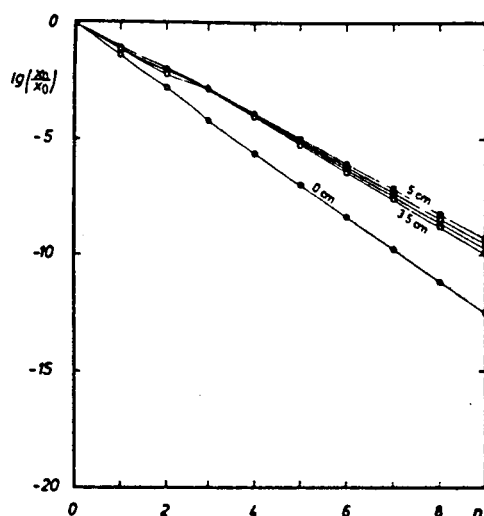


Fig. 4.2.-8

Trace of the occupation density distribution in a cross-current CO_2 -laser according to Jacoby [9] for the deformation oscillation of CO_2 at a spectral radiation density of 600 W/cm^2 with $\lambda = 10.5915 \mu\text{m}$.

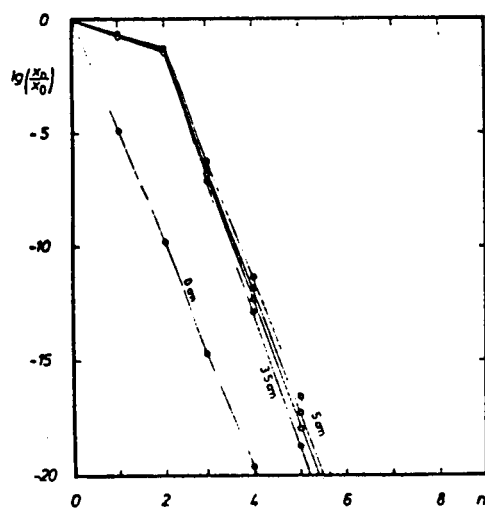


Fig. 4.2.-9

Trace of the occupation density distribution in a cross-current CO_2 -laser according to Jacoby [9] for the asymmetrical valence oscillation of CO_2 at a spectral radiation density of 600 W/cm^2 with $\lambda = 10.5915 \mu\text{m}$.

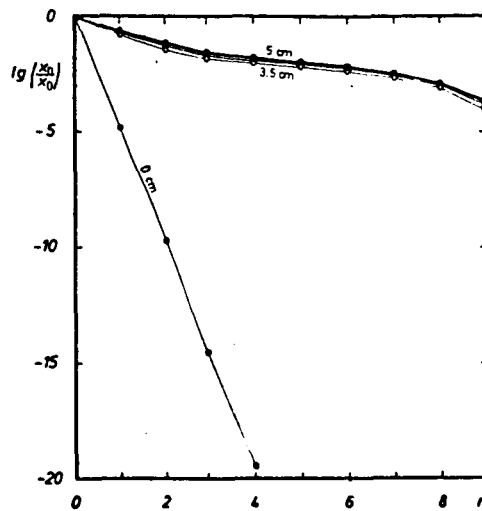


Fig. 4.2.-10

Trace of the occupation density distribution in a cross-current CO₂-laser according to Jacoby [9] for nitrogen at a spectral radiation density of 600 W/cm² with $\lambda = 10.5915 \mu\text{m}$.

4.3 Inversions in Compression Flow.

Due to the sometimes very different collision excitation rates of the vibrational degrees of freedom of CO₂ with other gas particles, one can suspect that, at rapid compressions of CO₂-containing gas mixtures, there can arise inversions between two rotational vibration states which are in contact with one another by means of a radiation crossing. Gases suffer rapid compressions, for example, at the passing of gas-dynamic collisions. The relationship of the state before the collision and the state after the collision is given by the Rankine-Hugoniot equations. Experiments show that in a wide region for the collision mach number, the translation-rotation relaxation zone and the vibrational relaxation zone are markedly separated from one another. Using the adiabatic exponent $\kappa = 7/5$ and with the help of the Rankine-Hugoniot equations, one obtains the state prior to the vibrational relaxation. Losev [13] gives two radiation crossings in which inversions are to be expected in the vibrational relaxation zone after a collision with a collision Mach number of $\text{Ma} = 4$ at

the initial pressure of $p_1 = 6$ Torr in a gas mixture of 10% CO_2 , 88% N_2 , and 2% H_2O . Here we deal with the crossings $04^0 0 \rightarrow 00^0 1$ and $20^0 0 \rightarrow 00^0 1$. The corresponding wavelengths lie at $50 \mu\text{m}$ and $22 \mu\text{m}$. Losev gives measurements which show that the expected inversions actually take place. With the help of a simplified model, Losev also obtains inversions numerically for these radiation crossings. The results of these calculations, however, don't agree too well with the results of the experiments. Losev explains this with the very short measuring times for the collision tube experiments and the measuring errors which become possible due to the cut-off at such large wavelengths.

The kinetic model used for this paper, was then used for the previously described collision tube flow. The results of these calculations and the results by Losev are compared to one another in Fig. 4.3.-1. One can see that the results of the model at hand agree better with the measurements than the results of the model by Losev.

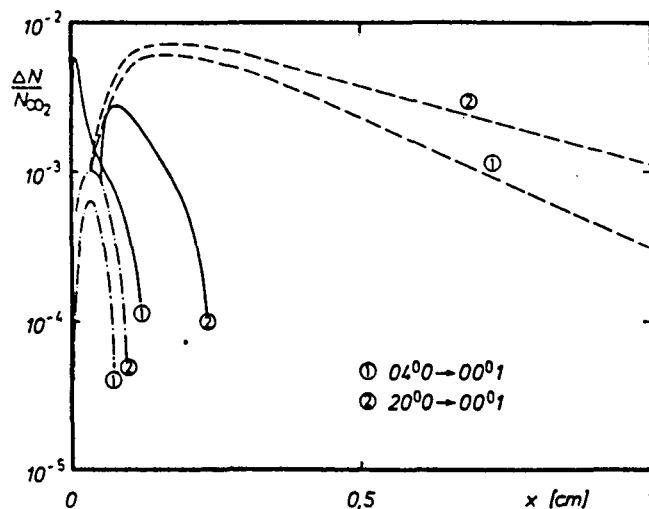


Fig. 4.3.-1

Trace of the occupation density difference for the crossings $04^0 0 \rightarrow 00^0 1$, P32 with $\lambda = 50.1940 \mu\text{m}$ and $00^0 0 \rightarrow 00^0 1$, P32 with $\lambda = 22.3210 \mu\text{m}$ after a collision with collision mach number $\text{Ma} = 4$, initial pressure of 8 mbar in 10% CO_2 - 2% H_2O - 88% N_2 .

— model at hand,
 ----- model by Losev [13],
 . - . - . measurements by Losev.

The better results with the model at hand can be taken back to the considerations of disturbances in the Boltzmann distribution. Fig. 4.3.-2 shows the deviation in the oscillation temperatures for the individual energy levels of CO_2 (ν_3) in contrast to the median vibration temperature for the total degree of freedom. The Boltzmann distributions for the remaining vibrational degrees of freedom don't appear to be markedly disturbed.

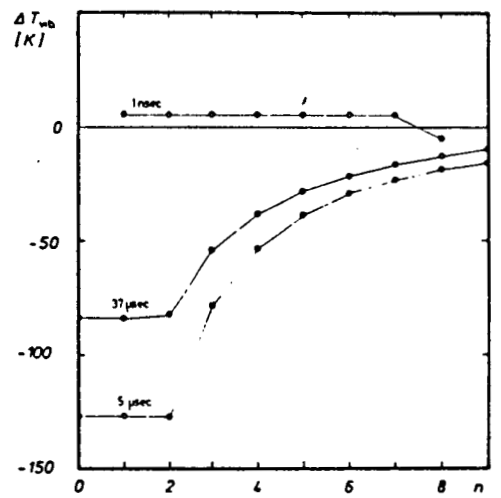


Fig. 4.3.-2

Deviation in the vibration temperature of the individual energy levels from the median vibration temperature for the asymmetrical valence oscillation of CO_2 after a collision with the collision mach number $\text{Ma} = 4$, initial pressure of 8 mbar in 10% CO_2 - 2% H_2O - 88% N_2 .

5. Summary

A kinetic model for the vibrational energy exchange in flowing gas mixtures was presented. In contrast to earlier models, no Boltzmann distribution was assumed for the occupation density distribution within the individual vibrational degrees of freedom. With the help of this model, the occurrences in certain gas-dynamic lasers and in the relaxation zone after gas-dynamic collisions can be described. The model was checked with known data for a cross-current CO_2 -laser with high-frequency excitation. The results of these calculations agree very well with the experimental results which were gained for the CO_2 -laser. In this context, we could show that the occupation density distributions of the individual vibrational degrees of freedom cannot be described by Boltzmann distributions. We could, furthermore, show that, upon discharge of this cross-current CO_2 -laser above the $9.6\text{ }\mu\text{m}$ - and the $10.6\text{ }\mu\text{m}$ -line, the prerequisites for the activation of a $16\text{ }\mu\text{m}$ - and a $14\text{ }\mu\text{m}$ -laser can be created. Finally, an investigation was made into whether or not one can expect inversions in the relaxation zone after gas-dynamic collisions. For this, it was shown by two examples that this is possible.

Appendix

A Reaction Velocity Constants

For the kinetic model at hand, 44 reaction velocity constants were needed. From literature, for about one half of the constants experimental results are known which span a wide temperature region. For 9 constants, the Millikan-White-Systematics could be utilized. Of these, 4 constants are covered by measured data for some temperatures. There still remain 12 velocity constants for VT-reactions which have to be determined in a theoretical manner. Of all theories mentioned in Chapter 3.2., the theory of Widom [14] best reproduces the velocity constants for VT-reactions for which there are experimental results available. Therefore, the theory of Widom is used to determine those constants for which there are no experimental results available.

A - 1 Experimentally Determined Constants

According to Chapter 3.2. , the expression

$$\ln \hat{k} = A + B \cdot T^{-1/3} + C \cdot T^{-2/3}$$

is used for VT-reactions. From experimental results, one obtains the coefficients which are listed in Table A - 1 . For VV- and for V-reactions the expression

$$\ln \hat{k} = A + B \cdot \sqrt{T} + C \cdot (\sqrt{T})^2$$

is used. From experimental results, one obtains the coefficients which are listed in Table A - 2 . The sources for the experimental results are given, sorted according to reactions in a special literature list at the end of this paper.

Reaction Equation	A	B	C
$\text{CO}_2^{(0)}(\nu_1) + \text{CO}_2 + 1388 \text{ cm}^{-1} \rightleftharpoons \text{CO}_2^{(1)}(\nu_1) + \text{CO}_2$	43,84	-251,79	748,34
$\text{CO}_2^{(0)}(\nu_2) + \text{CO}_2 + 667 \text{ cm}^{-1} \rightleftharpoons \text{CO}_2^{(1)}(\nu_2) + \text{CO}_2$	39,26	-189,64	485,89
$\text{CO}_2^{(0)}(\nu_2) + \text{H}_2\text{O} + 667 \text{ cm}^{-1} \rightleftharpoons \text{CO}_2^{(1)}(\nu_2) + \text{H}_2\text{O}$	28,18	11,51	0
$\text{CO}_2^{(0)}(\nu_2) + \text{He} + 667 \text{ cm}^{-1} \rightleftharpoons \text{CO}_2^{(1)}(\nu_2) + \text{He}$	29,04	-29,89	46,05
$\text{CO}_2^{(0)}(\nu_3) + \text{CO}_2 + 2349 \text{ cm}^{-1} \rightleftharpoons \text{CO}_2^{(1)}(\nu_3) + \text{CO}_2$	34,63	-92,1	0
$\text{CO}_2^{(0)}(\nu_3) + \text{N}_2 + 2349 \text{ cm}^{-1} \rightleftharpoons \text{CO}_2^{(1)}(\nu_3) + \text{N}_2$	25,50	126,7	-1329,0
$\text{H}_2\text{O}^{(0)}(\nu_2) + \text{H}_2\text{O} + 1595 \text{ cm}^{-1} \rightleftharpoons \text{H}_2\text{O}^{(1)}(\nu_2) + \text{H}_2\text{O}$	38,25	-80,5	34,54
$\text{H}_2\text{O}^{(0)}(\nu_2) + \text{N}_2 + 1595 \text{ cm}^{-1} \rightleftharpoons \text{H}_2\text{O}^{(1)}(\nu_2) + \text{N}_2$	31,34	-58,72	0
$\text{H}_2\text{O}^{(0)}(\nu_2) + \text{He} + 1595 \text{ cm}^{-1} \rightleftharpoons \text{H}_2\text{O}^{(1)}(\nu_2) + \text{He}$	40,16	-229,8	921
$\text{N}_2^{(0)} + \text{H}_2\text{O} + 2331 \text{ cm}^{-1} \rightleftharpoons \text{N}_2^{(1)} + \text{H}_2\text{O}$	33,96	-131,92	347,69
$\text{N}_2^{(0)} + \text{N}_2 + 2331 \text{ cm}^{-1} \rightleftharpoons \text{N}_2^{(1)} + \text{N}_2$	44,76	-388,7	1093,7
$\text{N}_2^{(0)} + \text{He} + 2331 \text{ cm}^{-1} \rightleftharpoons \text{N}_2^{(1)} + \text{He}$	39,24	-184,21	0
$\text{O}_2^{(0)} + \text{O}_2 + 1556 \text{ cm}^{-1} \rightleftharpoons \text{O}_2^{(1)} + \text{O}_2$	42,99	-274,58	575,65
$\text{O}_2^{(0)} + \text{He} + 1556 \text{ cm}^{-1} \rightleftharpoons \text{O}_2^{(1)} + \text{He}$	38,89	-180,52	383,89

Table A - 1

Experimentally determined coefficients for the reaction velocity constants of VT-reactions.

Reaction Equation

	A	B	C
$\text{CO}_2^{(0)}(\nu_3) + \text{N}_2^{(1)} + 18 \text{ cm}^{-1} \rightleftharpoons \text{CO}_2^{(1)}(\nu_3) + \text{N}_2^{(0)}$	29,93	-0,2756	$0,4934 \cdot 10^{-2}$
$\text{CO}_2^{(2)}(\nu_3) + \text{N}_2^{(0)} + 7 \text{ cm}^{-1} \rightleftharpoons \text{CO}_2^{(1)}(\nu_3) + \text{N}_2^{(1)}$	28,09	-0,06731	$0,983 \cdot 10^{-3}$
$\text{N}_2^{(0)} + \text{O}_2^{(1)} + 775 \text{ cm}^{-1} \rightleftharpoons \text{N}_2^{(1)} + \text{O}_2^{(0)}$	9,37	0,3723	$-0,1992 \cdot 10^{-2}$
$\text{N}_2^{(0)} + \text{H}_2\text{O}^{(1)}(\nu_2) + 736 \text{ cm}^{-1} \rightleftharpoons \text{N}_2^{(1)} + \text{H}_2\text{O}^{(0)}(\nu_2)$	11,63	0,303	0
$\text{CO}_2^{(3)}(\nu_3) + \text{CO}_2 + 416 \text{ cm}^{-1} \rightleftharpoons \text{CO}_2^{(1)}(\nu_3) + \text{CO}_2$	18,53	0,1855	$0,228 \cdot 10^{-2}$
$\text{CO}_2^{(3)}(\nu_3) + \text{H}_2\text{O} + 416 \text{ cm}^{-1} \rightleftharpoons \text{CO}_2^{(1)}(\nu_3) + \text{H}_2\text{O}$	19,42	0,2346	$-0,3615 \cdot 10^{-2}$
$\text{CO}_2^{(3)}(\nu_3) + \text{N}_2 + 416 \text{ cm}^{-1} \rightleftharpoons \text{CO}_2^{(1)}(\nu_3) + \text{N}_2$	23,09	-0,2719	$0,115 \cdot 10^{-1}$
$\text{CO}_2^{(3)}(\nu_3) + \text{O}_2 + 416 \text{ cm}^{-1} \rightleftharpoons \text{CO}_2^{(1)}(\nu_3) + \text{O}_2$	16,63	0,2915	0
$\text{CO}_2^{(3)}(\nu_3) + \text{He} + 416 \text{ cm}^{-1} \rightleftharpoons \text{CO}_2^{(1)}(\nu_3) + \text{He}$	16,6	0,2351	$0,1287 \cdot 10^{-2}$

Table A - 2

Experimentally determined coefficients for the reaction velocity constants of VV- and V-reactions.

A - 2 Application of the Millikan-White Systematics

For a string of reactions, there are either only a few direct experimental results, or only experimental results for the same reaction with other collision partners. For these cases, the MW-Systematics can be used if one doesn't expect any anomalous temperatures for the respective reactions. With Equations (2.3.1.-2.) and (3.1.-2.), one obtains

$$\ln \hat{k} = A + \ln \left[\frac{T}{1 - \exp(-\Theta/T)} \right] - B \cdot T^{-1/3}$$

with the expressions

$$A = 36,64 + 1,74 \cdot 10^{-5} \cdot \Theta^{4/3} \cdot \mu^{3/4}$$

$$B = 1,16 \cdot 10^{-3} \cdot \mu \cdot \Theta^{4/3}$$

for the coefficients so that k receives the units $\text{cm}^3/\text{mole}\cdot\text{sec}$. An estimate shows that the second term of the defining equation for A is generally small against the first constant term. A is, therefore, nearly independent of μ and Θ . A check with the help of experimental results shows that the MW-Systematics theory can be applied, in a few cases, to multi-atomic molecular gases, if the first constant term of the defining equation is fitted for A itself. In Table A - 3, the constants for those reactions are listed which can be handled with the help of the MW-Systematics.

Reaction Equation

	Θ [K]	A	B	
$\text{CO}_2^{(0)}(\nu_1) + \text{He} + 1388 \text{ cm}^{-1} \rightleftharpoons \text{CO}_2^{(1)}(\nu_1) + \text{He}$	1998	23,72	55,9	1)
$\text{CO}_2^{(0)}(\nu_2) + \text{N}_2 + 667 \text{ cm}^{-1} \rightleftharpoons \text{CO}_2^{(1)}(\nu_2) + \text{N}_2$	960	23,72	45,45	1)
$\text{CO}_2^{(0)}(\nu_2) + \text{O}_2 + 667 \text{ cm}^{-1} \rightleftharpoons \text{CO}_2^{(1)}(\nu_2) + \text{O}_2$	960	23,81	47,3	1)
$\text{CO}_2^{(0)}(\nu_3) + \text{He} + 2349 \text{ cm}^{-1} \rightleftharpoons \text{CO}_2^{(1)}(\nu_3) + \text{He}$	3381	24,9	112,72	1)
$\text{CO}_2^{(2)}(\nu_2) + \text{CO}_2 + 102 \text{ cm}^{-1} \rightleftharpoons \text{CO}_2^{(1)}(\nu_1) + \text{CO}_2$	147	16,72	4,2113	2)
$\text{CO}_2^{(2)}(\nu_2) + \text{H}_2\text{O} + 102 \text{ cm}^{-1} \rightleftharpoons \text{CO}_2^{(1)}(\nu_1) + \text{H}_2\text{O}$	147	16,67	3,2167	1)
$\text{CO}_2^{(2)}(\nu_2) + \text{N}_2 + 102 \text{ cm}^{-1} \rightleftharpoons \text{CO}_2^{(1)}(\nu_1) + \text{N}_2$	147	16,69	3,7228	2)
$\text{CO}_2^{(2)}(\nu_2) + \text{O}_2 + 102 \text{ cm}^{-1} \rightleftharpoons \text{CO}_2^{(1)}(\nu_1) + \text{O}_2$	147	16,7	3,8736	1)
$\text{CO}_2^{(2)}(\nu_2) + \text{He} + 102 \text{ cm}^{-1} \rightleftharpoons \text{CO}_2^{(1)}(\nu_1) + \text{He}$	147	14,81	3,2998	2)

Table A - 3

Constants for reaction velocity constants which are determined according to the MW-Systematics.

- 1) MW-Systematics applies to the same reaction with other reaction partners for which there are experimental results.
- 2) MW-Systematics was adjusted to the few available experimental data by varying A . With this correction, the other constants for the same reaction with other collision partners can be described for which there are more experimental results available.

Reactions with H_2O as a neutral or a reactive collision partner with the help of the MW-Systematics, are not too well described. One exception, however, is the Fermi-Resonance reaction.

A - 3 Application of Widom's Theory

The velocity constants for which there were no experimental results available and which could also not be described by the systematics of Millikan, White, were then determined with the help of the theory of Widom [14]. The validity of this theory was confirmed by the application of reactions for which experimental results were available. This theory deals with the exact solution of the Schrödinger equation for Maxwell-potentials, meaning the interaction potential in the form of

$$V(r) = A/r^4$$

For the vibrational relaxation time, one thus obtains

$$\tau \cdot p = \frac{\hbar \cdot \sqrt{3k_0 \cdot \kappa^5}}{32\pi^2 \cdot \gamma^2} \cdot \frac{m}{\mu} \cdot e^{-2\sqrt{2\frac{k_0}{\kappa}}} \cdot \cos^{-2}\left(\sqrt{2\frac{k_0}{\kappa}} + \frac{\pi}{8}\right) \cdot e^{-3\left(\gamma^2 \cdot \frac{k_T}{4\kappa}\right)^{2/3}}$$

if $k_0 \gg k_T \gg \kappa$ is satisfied. k_0 stands for a form of the crossing wave number which can be determined according to

$$\hbar^2 \cdot k_0^2 = 2\mu \cdot \epsilon_0 \quad \text{WITH} \quad \epsilon_0 = h \cdot c \cdot \bar{\nu}$$

where $\bar{\nu}$ is the actual emitted or absorbed wave number, if one deals with permitted crossings.

In the same sense, k_T stands for a thermal wave number which can be determined according to

$$\hbar^2 \cdot k_T^2 = 2\mu K \cdot T$$

where K stands for the Boltzmann constant. Quantity κ is a measure for the potential stiffness which is determined from A according to

$$\kappa = \hbar / \sqrt{2\mu A}$$

Therefore, this quantity also has the dimension of a wave number. Quantities μ and m stand for the reduced masses of collision and oscillation. Based on the relationship $A_{12}^2 = A_{11} \cdot A_{22}$, one obtains $\tilde{\kappa}$ at binary collisions from

$$\kappa^2 = \frac{M_1 + M_2}{2\sqrt{M_1 \cdot M_2}} \cdot \kappa_{11} \cdot \kappa_{22}$$

The values of κ for the individual molecular combinations are most reliably obtained from experimental results. Thus one can draw conclusions about the relaxation time of other molecular combinations for which there are no experimental results available, and which can also not be treated with the help of the MW-Systematics.

Combination	ν [cm ⁻¹]	$\bar{\mu}$ [g/mol]	m [g/mol]	κ [Å ⁻¹]
CO ₂ (ν ₁) - CO ₂	1388	22	8	4,98 *
H ₂ O	1388	12,7742	8	4,86
N ₂	1388	17,1111	8	4,91
O ₂	1388	18,5263	8	4,55
He	1388	3,6667	8	1,66
CO ₂ (ν ₂) - CO ₂	667	22	8,7273	3,19 *
H ₂ O	667	12,7742	8,7273	2,5 •
N ₂	667	17,1111	8,7273	3,93
O ₂	667	18,5263	8,7273	3,64
He	667	3,6667	8,7273	1,33 •
CO ₂ (ν ₃) - CO ₂	2349	22	8,7273	6,5 *
H ₂ O	2349	12,7742	8,7273	5,55
N ₂	2349	17,1111	8,7273	5,61 *
O ₂	2349	18,5263	8,7273	5,2
He	2349	3,6667	8,7273	1,9
H ₂ O (ν ₂) - CO ₂	1595	12,7742	1,7778	4,81
H ₂ O	1595	9	1,7778	4,3 •
N ₂	1595	10,9565	1,7778	3,54 *
O ₂	1595	11,52	1,7778	4,29
He	1595	3,2727	1,7778	1,99 •
N ₂ - CO ₂	2331	17,1111	7	4,87
H ₂ O	2331	10,9565	7	4,41 •
N ₂	2331	14	7	4,72 •
O ₂	2331	14,9333	7	4,4
He	2331	3,5	7	2,4 •
O ₂ - CO ₂	1556	18,5263	8	4,51
H ₂ O	1556	11,52	8	4,29
N ₂	1556	14,9333	8	4,4
O ₂	1556	16	8	4,1 *
He	1556	3,5556	8	1,9

Table A - 4

Molecular data which are needed for the application of the theory of Widom. Values for κ marked with an asterisk (*) were adjusted to experimental results for the reaction velocity constant.

For all degrees of freedom for CO_2 , the value $\kappa_{\text{He-He}} = 0.306 \text{ \AA}^{-1}$ was used which is calculated from $\text{CO}_2(\nu_2), \text{He}$ with the value $\kappa = 3.19 \text{ \AA}^{-1}$ for $\text{CO}_2(\nu_2), \text{CO}_2$. From other experimental results with He as a collision partner, one obtains a mean of

$$\kappa_{\text{He-He}} = 0,59 \text{ \AA}^{-1} .$$

Based on the structure of the CO_2 -molecule and its own vibrational form, one could expect that there would be a different value for κ for each vibrational degree of freedom. For reactions with CO_2 as collision partner, the arithmetic mean of all three values of κ was used as the parameter. It is

$$\kappa_{\text{CO}_2-\text{CO}_2} = 4,89 \text{ \AA}^{-1} .$$

As a result of the factor $\cos^{-2} \left(-\frac{\pi}{8} + \sqrt{2 - \frac{\kappa_0}{\kappa}} \right)$, the relaxation time for certain κ -values grows beyond all limits. For many molecular combinations, κ lies in the vicinity of such poles so that the relaxation time is very sensitive to small changes in κ .

The paths of the reaction velocity constants thus determined, are adjusted to a curve in the form of

$$\ln \hat{k} = A + B \cdot T^{-1/3} + C \cdot T^{-2/3}$$

with the help of the least squares method. For the still missing reactions, one obtains the coefficients A , B , and C in accordance with Table A - 5.

Reaction Equation	A	B	C
$\text{CO}_2^{(0)}(\nu_1) + \text{H}_2\text{O} + 1388 \text{ cm}^{-1} \rightleftharpoons \text{CO}_2^{(1)}(\nu_1) + \text{H}_2\text{O}$	42,85	- 201,5	582,6
$\text{CO}_2^{(0)}(\nu_1) + \text{N}_2 + 1388 \text{ cm}^{-1} \rightleftharpoons \text{CO}_2^{(1)}(\nu_1) + \text{N}_2$	42,75	- 211,5	613,9
$\text{CO}_2^{(0)}(\nu_1) + \text{O}_2 + 1388 \text{ cm}^{-1} \rightleftharpoons \text{CO}_2^{(1)}(\nu_1) + \text{O}_2$	41,94	- 220,9	641,2
$\text{CO}_2^{(0)}(\nu_3) + \text{H}_2\text{O} + 2349 \text{ cm}^{-1} \rightleftharpoons \text{CO}_2^{(1)}(\nu_3) + \text{H}_2\text{O}$	38,37	- 169,9	478,9
$\text{CO}_2^{(0)}(\nu_3) + \text{O}_2 + 2349 \text{ cm}^{-1} \rightleftharpoons \text{CO}_2^{(1)}(\nu_3) + \text{O}_2$	37,17	- 191,0	543,1
$\text{H}_2\text{O}^{(0)}(\nu_2) + \text{CO}_2 + 1595 \text{ cm}^{-1} \rightleftharpoons \text{H}_2\text{O}^{(1)}(\nu_2) + \text{CO}_2$	43,23	- 197,0	572,9
$\text{H}_2\text{O}^{(0)}(\nu_2) + \text{O}_2 + 1595 \text{ cm}^{-1} \rightleftharpoons \text{H}_2\text{O}^{(1)}(\nu_2) + \text{O}_2$	43,21	- 201,4	585,0
$\text{N}_2^{(0)} + \text{CO}_2 + 2331 \text{ cm}^{-1} \rightleftharpoons \text{N}_2^{(1)} + \text{CO}_2$	38,44	- 193,8	552,6
$\text{N}_2^{(0)} + \text{O}_2 + 2331 \text{ cm}^{-1} \rightleftharpoons \text{N}_2^{(1)} + \text{O}_2$	39,48	- 195,8	559,9
$\text{O}_2^{(0)} + \text{CO}_2 + 1556 \text{ cm}^{-1} \rightleftharpoons \text{O}_2^{(1)} + \text{CO}_2$	38,33	- 217,5	630,5
$\text{O}_2^{(0)} + \text{H}_2\text{O} + 1556 \text{ cm}^{-1} \rightleftharpoons \text{O}_2^{(1)} + \text{H}_2\text{O}$	41,98	- 202,8	588,9
$\text{O}_2^{(0)} + \text{N}_2 + 1556 \text{ cm}^{-1} \rightleftharpoons \text{O}_2^{(1)} + \text{N}_2$	41,31	- 211,0	610,4

Table A - 5

Coefficients of reaction velocity constants which were calculated according to the theory of Widom.

B Electrical Impulse Coefficients

The velocity spectrum of the electrons in the HF-impulse path of the laser cannot be described accurately enough by a Maxwell distribution with a translational temperature. For the total of all the electrons, there are deviations from a Maxwell distribution whose magnitude depends on the electron energy. An attempt is now made to describe the velocity spectrum of the electrons with the help of a Maxwell distribution which has two temperature parameters. For this, one electron temperature each is defined in the direction of the field lines, and the other electron temperature is defined perpendicular thereto, so that the valid distribution function is

$$f_e(\vec{v}) = \frac{\beta_{xy}^2}{\pi} \cdot \frac{\beta_z}{\pi} \cdot e^{-\beta_{xy}^2 \cdot (v_x^2 + v_y^2)} \cdot e^{-\beta_z^2 \cdot v_z^2}$$

with the coefficients

$$\beta_{xy}^2 = m / (2 K \cdot T_{xy}) \quad \text{and} \quad \beta_z^2 = m / (2 K \cdot T_z) \quad .$$

The velocity distribution of the molecules is described by the Maxwell distribution

$$f_M(\vec{w}) = (Y/\pi)^3 \cdot \exp(-Y^2 \cdot \langle \vec{w}, \vec{w} \rangle)$$

with the coefficients

$$Y^2 = M / (2 K T_0) \quad .$$

The relative velocity between a molecule and an electron is

$$g = \sqrt{\langle \vec{v} - \vec{w}, \vec{v} - \vec{w} \rangle} \quad .$$

When the electron temperature in the direction of the field lines (z-axis) is much greater than that perpendicular thereto, and is greater than the gas temperature, then the following relationship is valid as an approximation

$$g = v_z \quad .$$

The impulse coefficient is then obtained by

$$\vec{k}_{M,e} = \iiint_{-\infty}^{+\infty} \iiint_{-\infty}^{+\infty} 4 \cdot Q(v_z) \cdot v_z \cdot f_e(\vec{v}) \cdot f_M(\vec{w}) d\vec{v} d\vec{w} \quad .$$

Here, Q stands for the effective cross section. After integration over \vec{w} , v_x , and v_y , one obtains

$$\vec{k}_{M,e} = \int_{-\infty}^{+\infty} 4 Q(v_z) \cdot v_z \cdot (\beta_z / \pi) \cdot \exp(-\beta_z^2 \cdot v_z^2) dv_z \quad .$$

The portion of electrons with a velocity between v_z and $v_z + dv_z$ is

$$d\xi = 2 (\beta_z \cdot v_z) \cdot \exp[-(\beta_z \cdot v_z)^2] d(\beta_z v_z)$$

The median electron energy is then

$$\bar{u} = m / (2 \beta_z^2) \cdot \int_0^{\infty} \xi^3 \cdot \exp(-\xi^2) d\xi = \frac{1}{2} k \cdot T_z \quad .$$

One obtains for the median electron energy in terms of eV units

$$\bar{u} = \frac{1}{2} \frac{k}{e} \cdot T_z \quad .$$

With this, one can express the impulse coefficient by

$$\vec{k}_{M,e} = \frac{4}{\sqrt{\pi}} \cdot \sqrt{\bar{u} \cdot e / m} \cdot \int_0^{\infty} Q(u) \cdot \exp(-\frac{1}{2} \cdot u / \bar{u}) d(u / \bar{u}) \quad . \quad (B-1)$$

The effective cross sections $Q(u)$ for the electron collision excitation were taken from literature [15, 16]. The impulse coefficients thus determined, are presented in Fig. B - 1. The traces found by Nighan [11], are given as a comparison in Fig. B - 1. Within the reference of generally acceptable accuracies for kinetic data, there is good agreement. Thus it

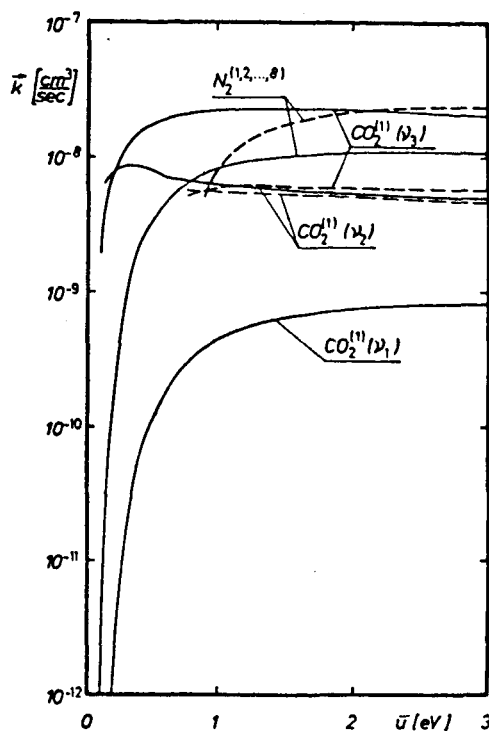


Fig. B - 1

Impulse coefficients for the vibrational degrees of freedom of CO_2 and N_2 due to electron collisions.

———— model at hand,

----- Nighan [11].

appears justified to drop the involved calculation of Nighan [11] and to determine the median kinetic parameters independent of one another.

With the help of Equation (B - 1), one obtains the kinetic parameters as they have been presented in Fig. B - 1 and B - 2. The impulse coefficients of all other levels and vibrational degrees of freedom can, on the other hand, be neglected.

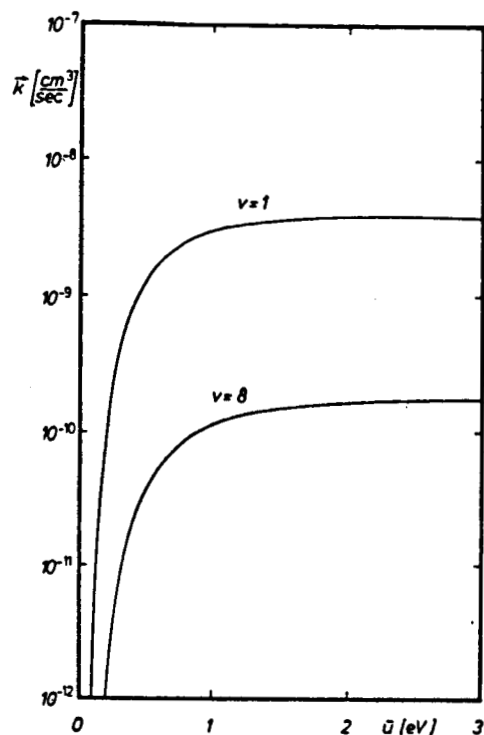
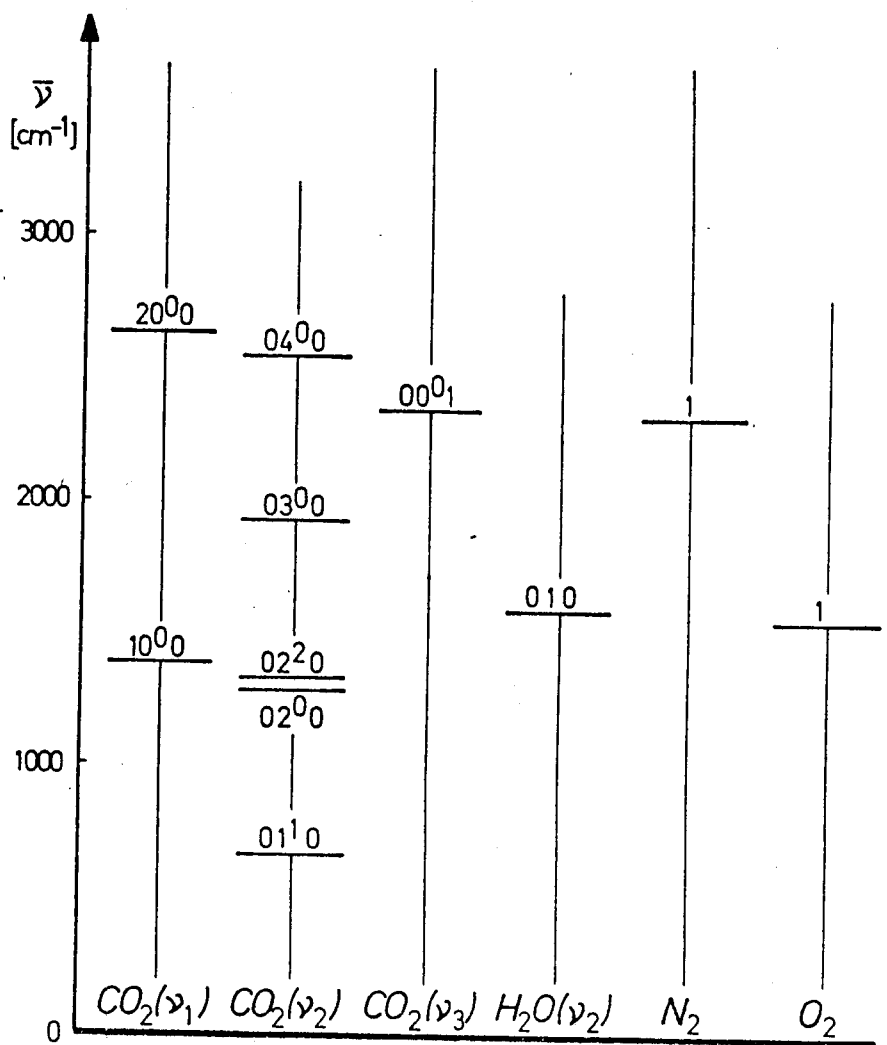


Fig. B - 2

Impulse coefficients for N_2 ($v=1$, $v=8$) according to theory under review.

C Term Scheme for the $\text{CO}_2 - \text{H}_2\text{O} - \text{N}_2 - \text{O}_2$ System



Literature Index:

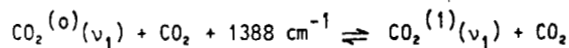
A special literature index for the kinetic data is given following this index.

Ein gesondertes Literaturverzeichnis für die kinetischen Daten befindet sich im Anschluß an dieses Verzeichnis.

- [1] Bethe, H.; Teller, E.
"Deviations from Thermal Equilibrium in Shock Waves"
Univ. of Mich. Eng. Res. Inst., Ann Arbor Mech. 1951
- [2] Döring, W.
"Einführung in die Quantenmechanik"
Göttingen, Vandenhoeck & Ruprecht 1962
- [3] Landau, L.; Teller, E.
Phys. Z. Sowiet., 10, 34 (1936)
- [4] Hurle, I.R.
"Vibrational Relaxation Processes under Conditions of Extreme Non-Equilibrium"
Chem. Soc. Spec. Publication No. 20
The Chem. Soc., Burlington House, London
Academic Press, London - New York, 1966
- [5] Johannesen, N.H.; Zienkiewicz, H.K.; Blythe, P.A.; Gerrard, J.H.
Physics of Fluids, 13, 213 (1962)
- [6] Taylor, R.L.; Rittnerman, S.
Rev. of Mod. Phys., 41, 26 (1969)
- [7] Blauer, J.A.; Nickerson, G.R.
"A Survey of Vibrational Relaxation Rate Data for Processes Important to CO₂-N₂-H₂O Infrared Plume Radiation"
AIAA Paper No. 74-536 ; AIAA 7th Fluid and Plasma Dyn. Conf.,
Palo Alto, Cal./ June 17-19, 1974
- [8] Millikan, R.C.; White, D.R.
J. Chem. Phys., 39, 3209 (1963)
- [9] Jacoby, H.
Forschungsbericht DFVLR Stuttgart
DFVLR-FB 83-06
- [10] Armandillo, E.; Kaye, A.S.
J. Phys. D: Appl. Phys., 13, 321 (1980)
- [11] Nighan, W.L.
Phys. Rev., A, 2, 1989 (1970)
- [12] Wexler, B.L.; Manuccia, T.J.; Waynant, R.W.
Appl. Phys. Lett., 31, 730 (1977)
- [13] Losev, S.A.
"Gasdynamic Laser"
Springer Series in Chemical Physics 12
Springer Verlag Berlin - Heidelberg - New York, 1981

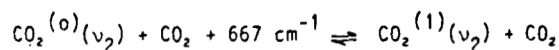
- [14] Widom, B.
J. Chem. Phys., 27, 940 (1957)
- [15] Schulz, G.J.
Phys. Rev., 135, A 988 (1964)
- [16] Boness, M.J.W.; Schulz, G.J.
Phys. Rev. Letters, 21, 1031 (1968)
- [17] Herzfeld, K.F.
J. Chem. Phys., 47, 743 (1967)
- [18] Kleen, W.; Müller, R.
"Laser"
Springer Verlag Berlin - Heidelberg - New York, 1969
- [19] Cottrell, T.L.; McCoubrey, J.C.
"Molecular Energy Transfer in Gases"
Butterworths London 1961
- [20] Offenhäuser, F.; Frohn, A.
"Theoretical and Experimental Study of
Vibrational Non-Equilibrium"
15th Int. Symp. Shock Waves and Shock Tubes, Berkeley 1985
- [21] Ryali, S.B.; Fenn, J.B.; Kolb, C.E.; Silver, J.A.
J. Chem. Phys., 76, 5878 (1982)
- [22] Herzfeld, K.F.; Litovitz, T.A.
Zeit. Phys., 156, 265 (1959)
- [23] Schwartz, R.N.; Herzfeld, K.F.
J. Chem. Phys., 22, 767 (1954)
- [24] Nikitin, Ye. Ye.
Optika i Spektrograf., 6, 141 (1959)
- [25] Novgorodov, M.Z.; Sviridov, A.G.; Sobolev, N.N.
IEEE J. Quant. Electr., 7, 508 (1971)

Literature index to the experimental results for the reaction velocity constants:



Buschmann, K.F.; Schäfer, K.
Zeitschr. f. Phys. Chem., B 50, 73 (1941)

Eckstrom, D.J.; Bershader, D.
J. Chem. Phys., 53, 2978 (1970)



Buschmann, K.F.; Schäfer, K.
Zeitschr. f. Phys. Chem., B 50, 73 (1941)

Camac, M.
Proc. Int. Symp. Fundament. Phen. Hypersonic Flow,
Cornell University 1966

Eucken, A.; Nümann, E.
Zeitschr. f. Phys. Chem., B 36, 163 (1937)

Carnevale, E.H.; Carey, C.; Larson, G.
J. Chem. Phys., 47, 2829 (1967)

Shields, F.D.
J. Acoust. Soc. Am., 29, 450 (1957)

• Shields, F.D.
J. Acoust. Soc. Am., 31, 248 (1959)

Daen, J.; de Boer, P.C.T.
J. Chem. Phys., 36, 1222 (1962)

Eckstrom, D.J.; Bershader, D.
J. Chem. Phys., 53, 2978 (1970)

Griffith, W.; Brickl, D.; Blackman, V.
Phys. Rev., 102, 1209 (1956)

Johannesen, N.H.; Zienkevich, H.K.; Blythe, P.A.; Gerrard, J.H.
Phys. Fluids, 13, 213 (1962)

van Itterbeek, A.; de Bruyn, P.; Mariëns, P.
Physica VI, 511 (1939)

van Itterbeek, A.; Mariëns, P.
Physica V, 153 (1938)

van Itterbeek, A.; Mariëns, P.
Physica VII, 125 (1940)

Simpson, C.J.S.M.; Bridgman, K.B.; Chandler, T.R.D.
J. Chem. Phys., 49, 513 (1968)

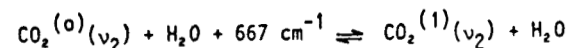
Simpson, C.J.S.M.; Chandler, T.R.D.; Strawson, A.C.
J. Chem. Phys., 51, 2214 (1969)

Küchler, L.
Zeitschr. f. Phys. Chem., B 41, 199 (1938)

Smiley, E.F.; Winkler, E.H.
J. Chem. Phys., 22, 2018 (1954)

Witteman, W.J.
J. Chem. Phys., 37, 655 (1962)

Weaner, D.; Roach, J.F.; Smith, W.R.
J. Chem. Phys., 47, 3096 (1967)



Buchwald, M.J.; Bauer, S.H.
J. Phys. Chem., 76, 3108 (1972)

van Itterbeek, A.; de Bruyn, P.; Mariëns, P.
Physica VI, 511 (1939)

van Itterbeek, A.; Mariëns, P.
Physica VII, 125 (1940)

Eucken, A.; Nümann, E.
Zeitschr. f. Phys. Chem., B 36, 163 (1937)

Smiley, E.F.; Winkler, E.H.
J. Chem. Phys., 22, 2018 (1954)

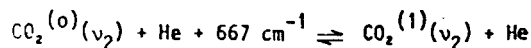
Knudsen, V.O.; Fricke, E.
J. Acoust. Soc. Am., 12, 255 (1940)

Gutowski, F.A.
J. Acoust. Soc. Am., 28, 478 (1956)

Lewis, J.W.; Lee, K.P.
J. Acoust. Soc. Am., 38, 813 (1965)

Eucken, A.; Becker, R.
Zeitschr. f. Phys. Chem., B 27, 235 (1934)

Higgs, R.W.; Torberg, R.H.
J. Acoust. Soc. Am., 42, 1038 (1967)

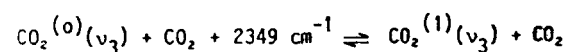


Eucken, A.; Nümann, E.
Zeitschr. f. Phys. Chem., B 36, 163 (1937)

Eucken, A.; Becker, R.
Zeitschr. f. Phys. Chem., B 27, 235 (1934)

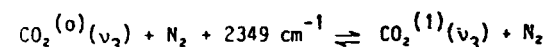
Küchler, L.
Zeitschr. f. Phys. Chem., B 41, 199 (1938)

Cottrell, T.L.; Day, M.A.
Chem. Soc. Spec. Publication No. 20
The Chem. Soc., Burlington House, London
Academic Press, London - New York 1966

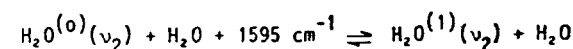


Gaydon, A.G.; Hurle, J.R.
8th Symp. on Comb. (Int.), 309 (1962)

Weaner, D.; Roach, J.F.; Smith, W.R.
J. Chem. Phys., 47, 3096 (1967)



Ryali, S.B.; Fenn, J.B.; Kolb, C.E.; Silver, J.A.
J. Chem. Phys., 76, 5878 (1982)



Bass, H.E.; Olson, J.R.; Amme, R.C.
J. Acoust. Soc. Am., 56, 1455 (1974)

Fujü, Y.; Lindsay, R.B.; Urushihara, K.
J. Acoust. Soc. Am., 35, 961 (1963)

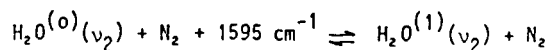
Huber, P.W.; Kantrowitz, A.
J. Chem. Phys., 15, 275 (1947)

Synofzik, R.
Diss. RWTH Aachen 1977

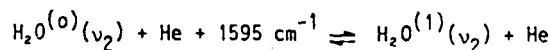
Kung, R.T.V.; Center, R.E.
J. Chem. Phys., 62, 2187 (1975)

Roesler, H.; Sahm, K.F.
J. Acoust. Soc. Am., 37, 386 (1965)

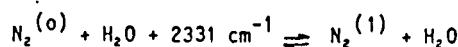
Eden, D.D.; Lindsay, R.B.; Zink, H.
J. Eng. Power, 1, 137 (1961)
Transactions of the ASME



Kung, R.T.V.; Center, R.E.
J. Chem. Phys., 62, 2187 (1975)



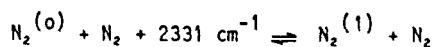
Kung, R.T.V.; Center, R.E.
J. Chem. Phys., 62, 2187 (1975)



Huber, P.W.; Kantrowitz, A.
J. Chem. Phys., 15, 275 (1947)

Center, R.E.; Newton, J.F.
J. Chem. Phys., 68, 3327 (1978)

Evans, L.B.
J. Acoust. Soc. Am., 51, 409 (1972)



Blackman, V.
J. Fluid Mech., 1, 61 (1956)

Gaydon, A.G.; Hurle, I.R.
8th Symp. on Comb. (Int.), 309 (1962)

Huber, P.W.; Kantrowitz, A.
J. Chem. Phys., 15, 275 (1947)

Lukasik, S.J.; Young, J.E.
J. Chem. Phys., 27, 1149 (1957)

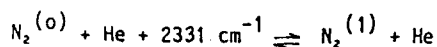
Millikan, R.C.; White, D.R.
J. Chem. Phys., 39, 98 (1963)

Hurle, I.R.
J. Chem. Phys., 41, 3911 (1964)

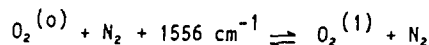
Appleton, J.P.
J. Chem. Phys., 47, 3231 (1967)

White, D.R.; Millikan, R.C.
AIAA Journ., 2, 1844 (1964)

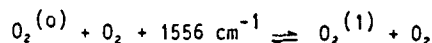
Bauer, H.J.; Roesler, H.
Chem. Soc. Spec. Publication No. 20
The Chem. Soc., Burlington House, London
Academic Press, London and New York, 1966



White, D.R.
J. Chem. Phys., 48, 525 (1968)



Bauer, H.J.; Roesler, H.
Chem. Soc. Spec. Publication No. 20
The Chem. Soc., Burlington House, London
Academic Press, London and New York, 1966



Blackman, V.
J. Fluid Mech., 1, 61 (1956)

van Itterbeek, A.; Mariens, P.
Physica VII, 125 (1940)

White, D.R.; Millikan, R.C.
J. Chem. Phys., 39, 1803 (1963)

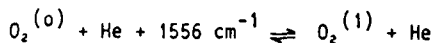
Losev, S.A.; Generalov, N.A.
Soviet Physics-Doklady, 6, 1081 (1962)

Holmes, R.; Smith, F.A.; Tempest, W.
Proc. Phys. Soc., 81, 311 (1963)

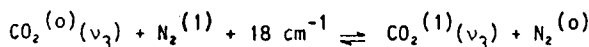
Shields, F.D.; Lee, K.P.
J. Acoust. Soc. Am., 35, 251 (1963)

Bauer, H.J.; Roesler, H.
Chem. Soc. Spec. Publication No. 20
The Chem. Soc., Burlington House, London
Academic Press, London and New York, 1966

Knötzel, H.; Knötzel, L.
Ann. d. Physik, 6(2), 393 (1948)



Millikan, R.C.; White, D.R.
J. Chem. Phys., 39, 3209 (1963)

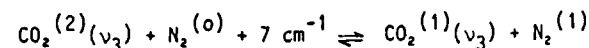


Rosser, W.A., Jr.; Wood, A.D.; Gerry, E.T.
J. Chem. Phys., 50, 4996 (1969)

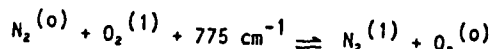
Taylor, R.L.; Bitterman, S.
J. Chem. Phys., 50, 1720 (1969)

Taylor, R.L.; Camac, M.; Feinberg, R.M.
Proc. 11th Symp. (Int.) Comb. 14-20 Aug. 1966
Comb. Inst., Pittsburg, Pa., 1967, S. 49

Gueguen, H.; Yzambart, F.; Chakroun, A.;
Margottin-Maclau, M.; Doyenette, L.; Henry, L.
Chem. Phys. Letters, 35, 198 (1975)

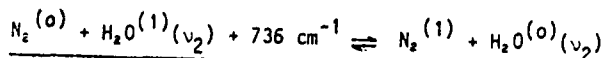


Pack, R.T.
J. Chem. Phys., 72, 6140 (1980)



Breshears, W.D.; Bird, P.F.
J. Chem. Phys., 48, 4768 (1968)

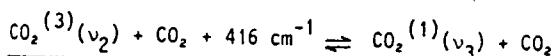
Bauer, H.J.; Roesler, H.
Chem. Soc. Special Publication No. 20
The Chem. Soc., Burlington House, London
Academic Press, London and New York, 1966



Whitson, M.E., Jr.; McNeal, R.J.
J. Chem. Phys., 66, 2696 (1977)

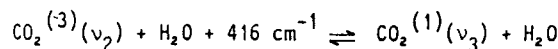
Kung, R.T.V.; Center, R.E.
J. Chem. Phys., 62, 2187 (1975)

Huber, P.W.; Kantrowitz, A.
J. Chem. Phys., 15, 275 (1947)

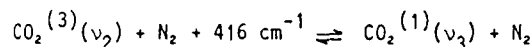


Rosser, W.A., Jr.; Wood, A.D.; Gerry, E.T.
J. Chem. Phys., 50, 4996 (1969)

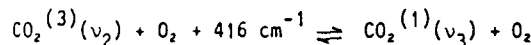
Hocker, L.O.; Kovacs, M.A.; Rhodes, C.K.
Phys. Rev. Letters, 47, 233 (1966)



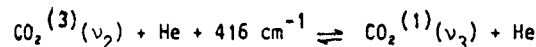
Rosser, W.A., Jr.; Gerry, E.T.
J. Chem. Phys., 51, 2286 (1969)



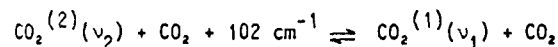
Rosser, W.A., Jr.; Wood, A.D.; Gerry, E.T.
J. Chem. Phys., 50, 4996 (1969)



Rosser, W.A., Jr.; Gerry, E.T.
J. Chem. Phys., 51, 2286 (1969)

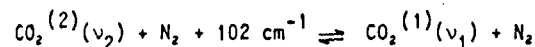


Rosser, W.A., Jr.; Gerry, E.T.
J. Chem. Phys., 51, 2286 (1969)

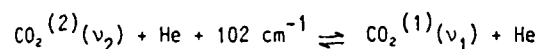


Rhodes, C.K.; Kelly, M.J.; Javan, A.
J. Chem. Phys., 48, 5730 (1968)

Jacobs, R.R.; Pettipiece, K.J.; Thomas, S.J.
Phys. Rev., A, 11, 54 (1975)



Jacobs, R.R.; Pettipiece, K.J.; Thomas, S.J.
Phys. Rev., A, 11, 54 (1975)



Jacobs, R.R.; Pettipiece, K.J.; Thomas, S.J.
Phys. Rev., A, 11, 54 (1975)

Curriculum Vitae

June 11, 1954	Born at Oberkirch/Ortenau County
April 1961 - June 1973	Attended grammar school and high school at Heidenheim/Brenz
June 1973	Graduated from high school
July 1973 - October 1974	Military service
October 1974 - April 1980	Studied air- and space technology at the University of Stuttgart. Employed as trainee and student worker with the following companies: <ul style="list-style-type: none">- J. M. Voith Co., Heidenheim/Brenz total of 6 months- Mecanica de la Peña S. A. , Urduliz total of 4 months
April 1980	Awarding of (University) diploma
since May 1980	Scientific employee at the Institut für Thermodynamik der Luft- und Raumfahrt an der Universität Stuttgart. (Institute for Thermodynamics of Air- and Space Travel at the University of Stuttgart).

END

DATE

JUN. 15, 1987